Design and Simulation of Broadband Microstrip Patch Radiator

A major thesis submitted to faculty of Technology

Of

University of Delhi

Towards the partial fulfillment of the requirement

For

The award of the degree

Master of Engineering

In

Electronics & Communication Engineering

Submitted By

Richa Joshi(Roll No.-4073)

Under the guidance of

Prof. Asok De

DEPARTMENT OF ELECTRONICS AND COMMUNICATION ENGINEERING

DELHI COLLEGE OF ENGINEERING

UNIVERSITY OF DELHI

DELHI-110042

(SESSION:2002-2005)

CERTIFICATE

This is to certify that the work entitled "Design and Simulation of Broadband Microstrip Patch Radiator" being submitted by **Richa Joshi** (Roll No. 4073) in partial fulfillment of the requirement for the degree of Master of Engineering in Electronics and Communication, Delhi College of Engineering, University of Delhi, Delhi, during the session 2002-2005 is a record of bonafide work done by her under our supervision and guidance. It is also certified that the dissertation has not been submitted elsewhere for any other degree.

Prof. ASOK DE
Project Guide
Head of Department
Deptt. of Information Technology
Delhi College of Engineering
Delhi

Prof. ASOK BHATTACHARYA
Head of Department
Deptt. of Electronics & Communication
Delhi College of Engineering
Delhi

ACKNOWLEDGEMENT

It is my pleasure to acknowledge and express my deep sense of gratitude towards my teacher and guide, **Prof. Asok De**, Professor and Head, Department of Information Technology, Delhi College of Engineering, who supervised the work reported in this major thesis report. He was always kind, cooperative and helped me whenever I needed his support. In spite of his busy schedule, he could find time to provide precious guidance and encouragement.

I would also like to thank Prof. Asok Bhattacharya, Head Deptt. of Electronics & Communication Engineering, Delhi College of Engineering, Delhi and Mr. N.S.Raghava, Senior Lecturer, Deptt. of Electronics & Communication Engineering, Delhi College of Engineering, Delhi for the support provided by them during the entire duration of degree & especially in this project.

I would like to thank the Governing Body of ITM, the college Director Prof. H.P. Garg, Prof. Swaran Ahuja (HOD, ECE Deptt., ITM, Gurgaon) and all my colleagues for their inspiration and continual help in this project.

Finally I thank everyone who has helped me either directly or indirectly in the successful completion of this work.

Richa Joshi
ME (E & C)
Class Roll.No.15/E & C/02
Univ. Roll No. 4073

TABLE OF CONTENTS

TABLE OF FIGURES

PREFACE

The concept of microstrip radiators was proposed in 1953. However, 20 years passed before practical antennas were fabricated. A microstrip radiator is essentially a printed circuit board with all of the power dividers, matching networks and phasing circuits, photo etched on one side of the board. The other side of board is a metal ground plane and thus the antenna can be directly applied to a metallic surface on an aircraft or missile. Development during the 1970s was accelerated by the availability of good substrates with low loss tangent and attractive thermal and mechanical properties, improved photolithographic techniques, and better theoretical models. Since then, extensive research and development of microstrip antennas and arrays, aimed at exploiting their numerous advantages such as light weight, low volume, low cost, conformal configuration, compatibility with integrated circuits, and so on, have to diversified applications and to the establishment of the topic as the separate entity with in the broad field of microwave antennas. Objectives of this project are;

- To analyze a basic rectangular microstrip patch antenna.
- To design a broadband v-shaped rectangular microstrip patch radiator for a particular set of parameters like substrate height, operating frequency etc.
- To study the software IE3D for its use in simulation of microstrip patch antennas.
- To model the designed antenna using IE3D and simulate it.
- To study the result obtained from the simulations.

1 INTRODUCTION

1.1 OVERVIEW OF ANTENNA

An antenna is defined as "a usually metallic device (as a rod or wire) for radiating or receiving radio waves". The *IEEE Standard Definitions of Terms for Antennas* defines the antenna or aerial as a "***means for radiating or receiving radio waves***". In other words the antenna is the transitional structure between free-space and a guiding device. The guiding device may take the form of a coaxial line or a waveguide, and is used to transport electromagnetic energy from the transmitting source to the antenna, or from the antenna to the receiver. Commonly used antennas are wire antennas, aperture antennas, array antennas, reflector antennas etc. To describe the performance of an antenna, definitions of various parameters are necessary. Some of the parameters are interrelated and not all of them need be specified for complete description of the antenna performance. Some prominent parameters are

Radiation pattern
An antenna radiation pattern or antenna pattern is defined as "a mathematical function or a graphical representation of the radiation properties of the antenna as a function of space coordinates".

Radiation intensity
The power radiated from an antenna per unit solid angle.

Directivity
The ratio of the radiation intensity in a given direction from the antenna to the radiation intensity averaged over all directions.

Gain
Absolute gain of an antenna (in a given direction) is defined as "the ratio of the intensity, in the given direction, to the radiation intensity that would be obtained if power accepted by the antenna were radiated isotropically**.**

Antenna Efficiency
The ratio of the power radiated (Pr) to the power fed into the antenna (P_T).
$\eta = (Pr/ P_T) X 100$

Halfpower Beamwidth
In a plane containing the direction of the maximum of a beam, the angle between the two directions in which the radiation intensity is one-half the maximum value of the beam.

1.2 MICROSTRIP ANTENNAS

Microstrip antenna consists of a radiating patch on one side of a dielectric substrate with a ground plane on the other side. In high performance aircraft, spacecraft, satellite and missile applications, where size, weight, cost, performance, ease of installation, and aerodynamic profile are constraints, and low profile antennas may be required. Presently there are many applications, such as mobile radio and wireless communications that have similar specifications. To meet these requirements, microstrip antennas can be used. These antennas are low profile, conformable to planar and nonplanar surfaces, simple and inexpensive to manufacture using printed circuit technology, mechanically robust when mounted on rigid surfaces, compatible with MMIC designs, and when the particular patch shape and mode are selected they are very versatile in terms of resonant frequency, polarization, pattern and impedance. In addition, by adding loads between the patch and ground plane, such as pins and varactor diodes, adaptive elements with variable resonant frequency, impedance, polarization and pattern can be designed.

Major operational disadvantages of microstrip antennas are their low efficiency, low power, high Q (sometimes in excess of 100), poor polarization purity, poor scan performance, spurious feed radiation and very narrow frequency bandwidth, which is typically only a fraction of a percent or at most a few percent. In some applications, such as government security systems, narrow bandwidths are required. However, there are methods, such as by increasing the height of the substrate, which can be used to extend the efficiency and bandwidth.

1.3 BASIC CHARACTERISTICS OF THE MICROSTRIP ANTENNA

As shown in figure 1.1 below, a microstrip antenna in its simplest configuration consists of a radiating patch on one side of a dielectric substrate which has a ground plane on the other side.

Microstrip antennas consist of a very thin ($t<<\lambda_0$ where λ_0 is the free space wavelength) metallic strip(patch) placed small fraction of a wavelength ($h<<\lambda_0$, usually $0.003\ \lambda_0 \leq h \leq 0.05\ \lambda_0$) above a ground plane. The microstrip patch is designed so its pattern maximum is normal to the patch (broadside radiator). This is accomplished by properly choosing the mode (field configurations) of excitation beneath the patch. End-fire radiation can also be accomplished by judicious mode selection.

For a rectangular patch, the length l of element is usually $\lambda 0/3 < l < \lambda 0/2$. The strip and the ground plane are separated by a dielectric sheet (referred to as the substrate), as shown in the figure 1.2.

There are numerous substrates that can be used for the design of microstrip antennas and their dielectric constants are usually in the range of $2.2 \leq \varepsilon r \leq 12$. The dielectric constant is in the lower end of the range because they provide better efficiency, larger bandwidth, loosely bound fields for radiation into space, but at the expense of larger element size.

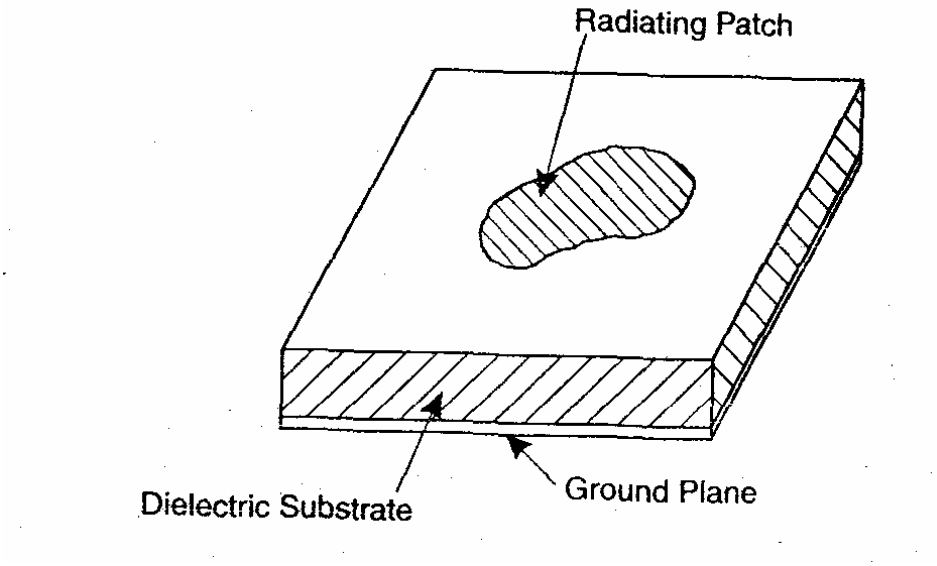

Figure1.1 Microstrip Antenna Configuration

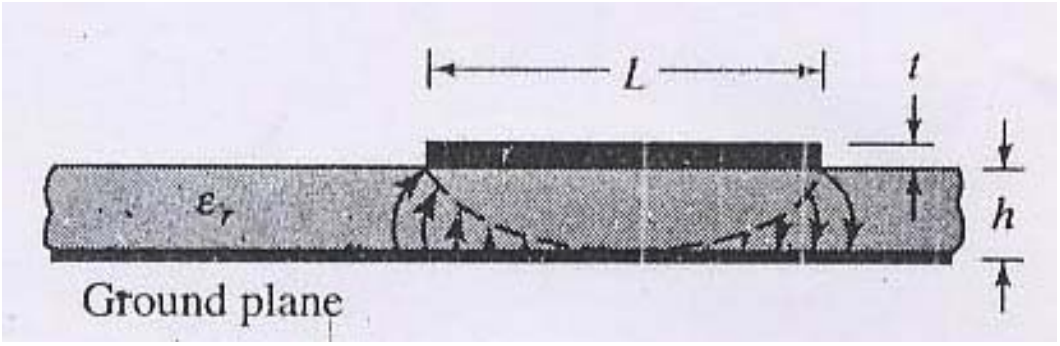

Figure 1.2 Side View of a Microstrip Antenna

Thin substrates with higher dielectric constants are desirable for microwave circuitry because they require tightly bound fields to minimize undesired radiation and coupling, and lead to smaller element sizes; however, because of their greater losses, they are less efficient and have relatively smaller bandwidths. Since microstrip antennas are often integrated with microwave circuitry, a compromise has to be reached between good antenna performance and circuitry design. Often microstrip antennas are also referred to as patch antennas. The radiating elements and the feed lines are usually photo etched on the dielectric substrate. The radiating patch may be square, rectangular, thin strip (dipole), circular, elliptical, triangular or any other configuration.

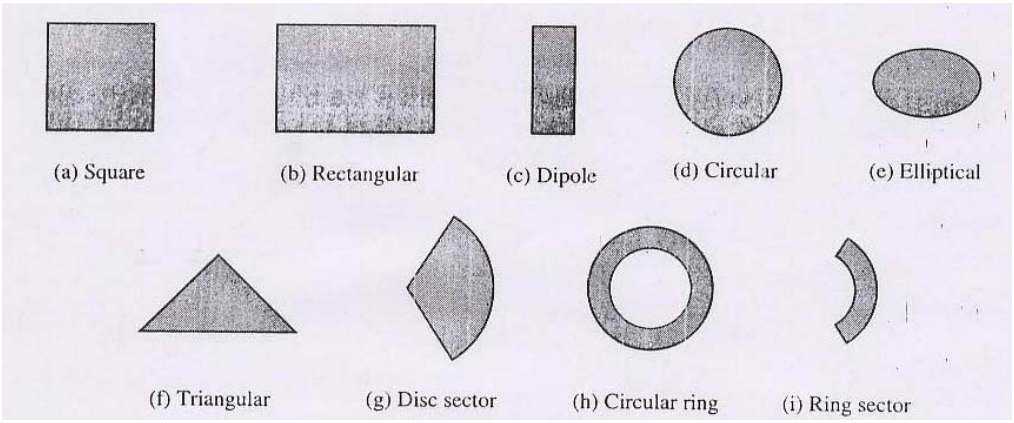

Figure1.3 Various Configurations of a Microstrip Patch

1.4 ADVANTAGES AND DISADVANTAGES OF MICROSTRIP ANTENNA

Microstrip antennas are increasing in popularity for use in wireless applications due to their low-profile structure. Therefore they are extremely compatible for embedded antennas in handheld devices such as cellular phones. Telemetry and communication antennas on missiles need to be thin and conformal and are often microstrip patch antennas. Another area where they have been used successfully is in satellite communication.

Some of their principal advantages are

- Light weight and low volume.
- Low profile planar configuration.
- Low fabrication cost.
- Supports both linear and circular polarization.
- Can be easily integrated with microwave integrated circuits (MICs).
- Capable of dual and triple frequency operations.
- Mechanically robust when mounted on rigid surfaces.
- The antennas may be easily mounted on missiles, rockets and satellites without major alterations.
- No cavity backing required.
- The antennas are compatible with modular designs.
- Feed line and matching networks are fabricated simultaneously with the antenna structure.

Microstrip antennas suffer from certain disadvantages like

- Narrow bandwidth.
- Low efficiency.
- Poor end-fire radiation.
- Low gain.
- Most microstrip antennas radiate into a half plane.
- Practical limitations on the maximum gain (approx. 20dB).
- Possibility of excitation of surface waves.
- Lower power handling capability.

But these disadvantages can be overcome by making design modifications in the basic structure.

2 ANALYSIS OF RECTANGULAR MICROSTRIP PATCH RADIATOR

2.1 INTRODUCTION

There are many methods of analysis for microstrip antennas. The most popular models are the transmission-line model, cavity model and full-wave model (which include primarily integral equations/Moment Method).

The transmission line model is easiest of all, it gives good physical insight, but is less accurate and it is more difficult to model coupling. Compared to transmission line model, the cavity model is more accurate but at the same time more complex. However, it gives good physical insight. In general when applied properly, the full-wave models are very accurate, very versatile, and can treat single elements, finite and infinite arrays, stacked elements, arbitrary shaped elements, and coupling. However they are the most complex models and usually give less physical insight.

In the present work we have analyzed the microstrip antenna using the cavity model due to its substantial advantages.

2.2 CAVITY MODEL

Microstrip antenna resembles dielectric loaded cavities, and they exhibit higher order resonances. The normalized fields within the dielectric substrate (between the patch and the ground plane) can be found more accurately by treating that region as a cavity bounded by electric conductors (above and below it) and by magnetic walls (to simulate an open circuit) along the perimeter of the patch. This is an approximate model, which in principle leads to a reactive input impedance (of zero or infinite value of resonance), and it does not radiate any power. However, assuming that the actual fields are approximate to those generated by such a model, the computed pattern, input admittance, and resonant frequencies compare well with measurements.

When the Microstrip patch is energized, a charge distribution is established on the upper and lower surfaces of the patch, as well as on the surface of the ground plane, as shown in figure 2.1.

The charge distribution is controlled by two mechanisms: *an attractive and a repulsive mechanism*. The attractive mechanism is between the corresponding opposite charges on the bottom side of the patch and the ground plane, which tends to maintain the charge on the bottom of the patch. The repulsive mechanism is between like charges on the bottom of surface of the patch, which tends to push some charges from the bottom of the patch, around its edges, to its top surface. The movement of these charges creates, corresponding current densities $\mathbf{J}_b$ and $\mathbf{J}_t$, at the bottom and the top surfaces of the patch, respectively, as shown in figure 2.1 .

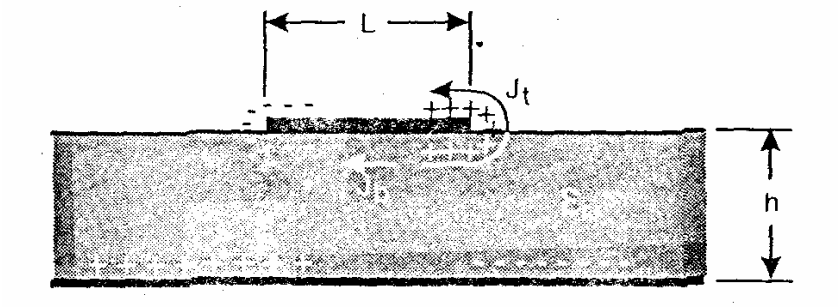

Figure2.1 Charge Distribution and Current Density Creation on a Microstrip Patch

Since for most practical microstrips the height to width ratio (*h/W)* is very small, the attractive mechanism dominates and most of the charge concentration and current flow remain underneath the patch. A small amount of current flows around the edges of the patch to its top surface. However this current flow decreases as the *h/W* ratio decreases. In the limit, the current flow to the top would be zero, which ideally would not create any tangential magnetic field components to the edges of the patch. This would allow the four side walls to be modeled by perfect magnetic conducting surfaces which ideally would not disturb the magnetic field and in turn the electric field distributions beneath the patch. Since in practice there is a finite height to width ratio, although small, the tangential magnetic fields at the edges would not be exactly zero. However, since they will be small, a good approximation to the cavity model is to treat the side walls as perfectly magnetic conducting. This model produces good normalized electric and magnetic field distributions (modes) beneath the patch.

If the microstrip antenna were treated only as a cavity, it would not be sufficient to find the absolute amplitudes of the electric and magnetic fields. In fact by treating the walls of the cavity, as well as the material within it as lossless, the cavity would not radiate and its input impedance would be purely reactive. To account for radiation, a loss mechanism has to be introduced, this is taken into account by radiation resistance R_r and loss resistance R_l. These two resistances allow the input impedances to be complex and for its functions to have complex poles; the imaginary poles representing, through R_r and R_l, the radiation and conduction dielectric losses. To make the microstrip lossy using the cavity model, which would then represent an antenna, the loss is taken into account by introducing an effective loss tangent δ_{eff}.. The effective loss tangent is chosen appropriately to represent the loss mechanism of the cavity, which now behaves as an antenna and is taken as the reciprocal of quality factor Q (δ_{eff}=1/Q).

Because the thickness of the microstrip is usually very small, the waves generated within the dielectric substrate (between the patch and the ground plane) undergo considerable reflections when they arrive at the edge of the patch. Therefore only a small fraction of the incident energy is radiated; thus the antenna is considered to be very inefficient. The fields beneath the patch form standing waves that can be represented by cosinusoidal wave functions. Since the height of the substrate is very small ($h << \lambda$ where λ is the wavelength within the dielectric), the field variation along the height will be considered constant. In addition, because of very small substrate height, the fringing of the fields along the edges of the patch are also very small

whereby the electric field is nearly normal to the surface of the patch. Therefore only $\mathbf{TM}_x$ field configurations will be considered within the cavity. While the top and the bottom of walls of the cavity are perfectly electric conducting, the four sidewalls will be modeled as perfectly conducting magnetic walls (tangential magnetic fields vanish along those four walls).

2.2.1 EQUIVALENT CURRENT DENSITIES

It has been shown using the cavity model that the microstrip antenna can be modeled reasonably well by a dielectric-loaded cavity with two perfectly conducting electric walls (top and bottom), and four perfectly conducting magnetic walls (sidewalls). It is assumed that the material of the substrate is truncated and does not extend beyond the edges of the patch. The four sidewalls represent four narrow apertures through which radiation takes place. Using Field Equivalence Principle (Huygen's Principle), the microstrip patch is represented by an equivalent electric current density $\mathbf{J}_t$ at the top surface of the patch to account for the presence of patch (there is also a current density $\mathbf{J}_b$ at the bottom of the patch which is no needed for this model). The four side slots are represented by the equivalent electric current density $\mathbf{J}_s$ and equivalent magnetic current density $\mathbf{M}_s$, as shown in figure 2.2(a)

$$\mathbf{J_s = n \; X \; H_a}$$

$$\mathbf{M_s = -n \; X \; E_a}$$

Where Ea and Ha represent, respectively, the electric and magnetic fields at the slots. Because it was shown that for microstrip antennas with very small height to width ratio the current density Jt at the top of the patch is much smaller than the current density J_b at the bottom of the patch, it will be assumed it is negligible here and it will be set to zero. Also it was argued that the tangential magnetic fields along the edge of the patch are very small, ideally zero. Therefore the corresponding equivalent electric current density Js will be very small (=0), and it will be set to zero here.

Thus the only nonzero current density is equivalent magnetic current density $\mathbf{M}_s$ along the side periphery of the cavity radiating in the presence of ground plane as shown in figure 2.2(b). The presence of the ground plane can be taken into account by image theory that will double the equivalent magnetic current density. Therefore the final equivalent is a magnetic current density of twice or $\mathbf{M_s = -2n \; X \; E_a}$ around the side periphery of the patch radiating into free space as shown in figure 2.2(c).

There are a total of four slots representing the microstrip antenna, only two (the radiating slots) account for most of the radiation; the fields radiated by the other two, which are separated by the width W of the patch, cancel along the principal planes. Therefore the same two slots, separated by the length of the patch, are referred to here as *radiating slots*. The two slots form a two-element array with a spacing of $\lambda/2$, where λ is the guide wavelength in the substrate, in order for the fields at the aperture of the two slots to have opposite polarization. In a direction perpendicular to the ground plane the components of the field add in phase and give a maximum radiation normal to the patch; thus broadside antenna.

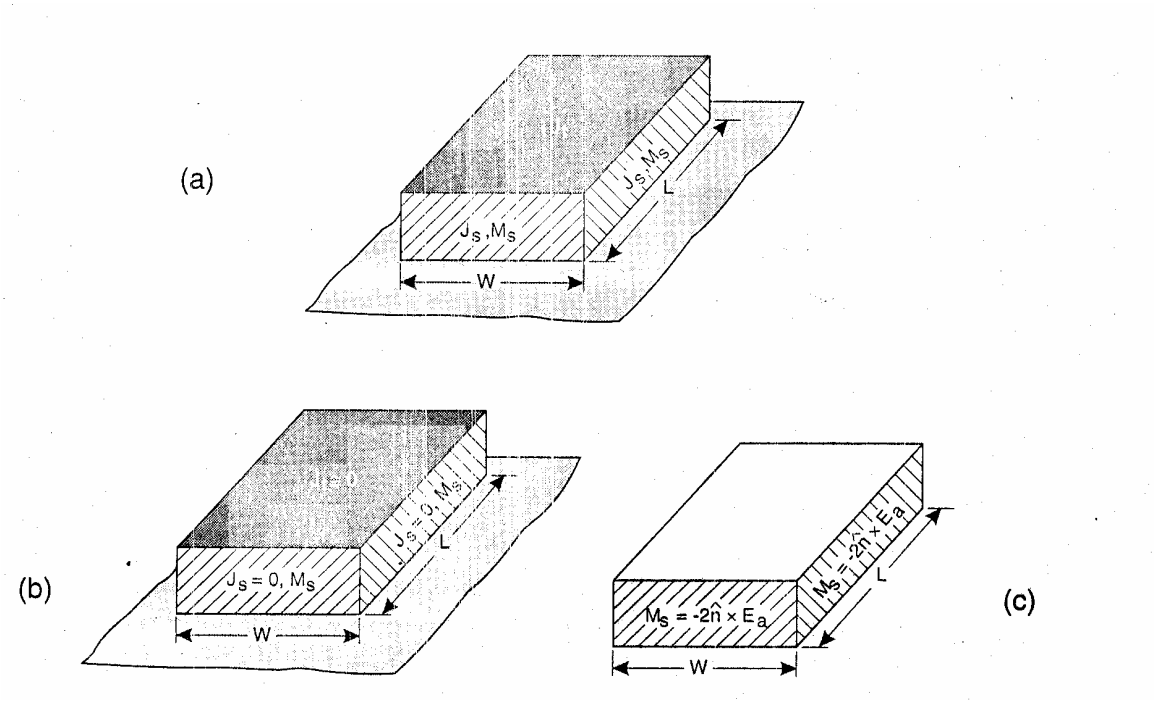

Figure2.2 Equivalent Current Densities on Four Sides of Rectangular Microstrip Patch

Using the equivalence principle, each slot radiates the same fields as a magnetic dipole with current densities **M**. By referring to *figure 2.3* the equivalent magnetic current densities along the two slots, each of width W and height h, are both of the same magnitude and of the same phase, and separated by L.

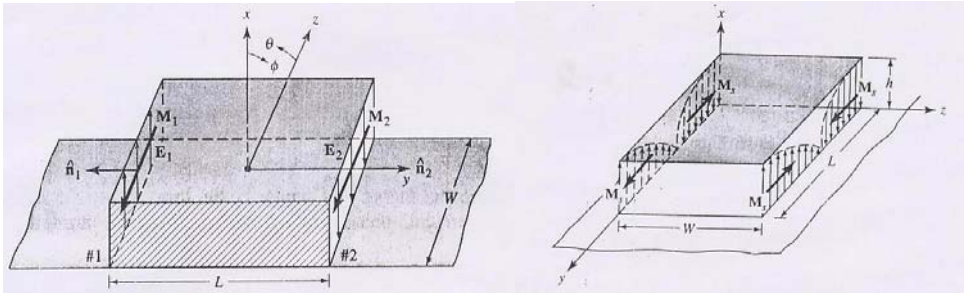

(a) (b)

Figure2.3: (a) Radiating Slots And Equivalent Magnetic Current Densities (b)Current Densities on Nonradiating Slots of Rectangular Microstrip Patch

Thus these two sources will add in a direction normal to the patch and ground plane forming a broadside pattern.

2.2.2 FIELD CONFIGURATIONS

The field configurations within the cavity can be found using the vector potential approach. The volume beneath the patch can be treated as a rectangular cavity loaded with a dielectric material of dielectric constant ε_r.

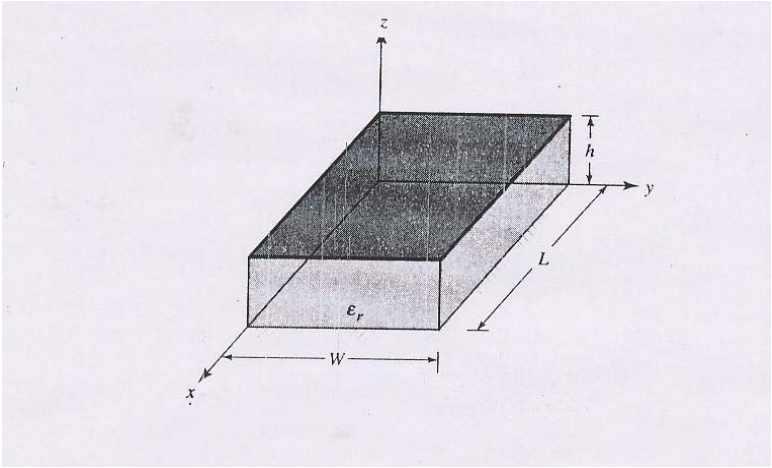

Figure2.4 Rectangular Microstrip Patch Geometry

The vector potential A_z must satisfy the homogeneous wave equation of

$$\nabla^2 \mathbf{A_z} + k^2 \mathbf{A_z} = 0$$

where

$$\mathbf{A_z} = \{A_1 \cos(k_x x) + B_1 \sin(k_x x)\}\{A_2 \cos(k_y y) + B_2 \sin(k_y y)\}\{A_3 \cos(k_z z) + B_3 \sin(k_z z)\}$$

k_x, k_y, k_z are wave numbers along the x, y and z directions. These will be determined subject to boundary conditions.

We know, $\mathbf{H_A} = \frac{1}{\mu} \nabla \times \mathbf{A}$

Here $\mathbf{A} = \mathbf{i}A_x + \mathbf{j}A_y + \mathbf{k}A_z \equiv \mathbf{k}A_z$

$$\nabla \times \mathbf{A} = \begin{vmatrix} \mathbf{i} & \mathbf{j} & \mathbf{k} \\ \partial/\partial x & \partial/\partial y & \partial/\partial z \\ A_x & A_y & A_z \end{vmatrix} = \mathbf{i}\left(\frac{\partial A_z}{\partial y}\right) - \mathbf{j}\left(\frac{\partial A_z}{\partial x}\right)$$

$\therefore$

$$H_x = \frac{1}{\mu}\frac{\partial A_z}{\partial y}$$

$$H_y = \frac{1}{\mu}\frac{\partial A_z}{\partial x}$$

$$H_z = 0$$

Also we have,

$$\mathbf{E_A} = -j\omega\ \mathbf{A} - \frac{j}{\omega\mu\varepsilon}\nabla(\nabla \cdot \mathbf{A})$$

$$\mathbf{A} = \mathbf{k}A_z$$

$$\nabla \cdot \mathbf{A} = \frac{\partial A_z}{\partial x}$$

$$\nabla(\nabla \cdot \mathbf{A}) = \mathbf{i}\frac{\partial^2 A_z}{\partial z \partial x} + \mathbf{j}\frac{\partial^2 A_z}{\partial z \partial y} + \mathbf{k}\frac{\partial^2 A_z}{\partial^2 z}$$

$$\mathbf{E_A} = \mathbf{i}E_x + \mathbf{j}E_y + \mathbf{k}E_z$$

$$\mathbf{E_A} = -j\omega\ \mathbf{k}A_z - \frac{j}{\omega\mu\varepsilon}\left(\mathbf{i}\frac{\partial^2 A_z}{\partial z \partial x} + \mathbf{j}\frac{\partial^2 A_z}{\partial z \partial y} + \mathbf{k}\frac{\partial^2 A_z}{\partial^2 z}\right)$$

Therefore,

$$E_x = -\frac{j}{\omega\mu\varepsilon}\frac{\partial^2 A_z}{\partial z \partial x}$$

$$E_y = -\frac{j}{\omega\mu\varepsilon}\frac{\partial^2 A_z}{\partial z \partial y}$$

$$E_z = -\frac{j}{\omega\mu\varepsilon}\left(\frac{\partial^2}{\partial z^2} + k^2\right)A_z$$

Boundary conditions:

$$E_x(0 \le x' \le L, 0 \le y' \le W, z' = 0) = E_x(0 \le x' \le L, 0 \le y' \le W, z' = h) = 0$$
$$H_x(0 \le x' \le L, y' = 0, 0 \le z' \le h) = H_x(0 \le x' \le L, y' = W, 0 \le z' \le h) = 0$$
$$H_y(x = 0, 0 \le y' \le W, 0 \le z' \le h) = H_y(x' = L, 0 \le y' \le W, 0 \le z' \le h) = 0$$

Substituting these boundary conditions into the field equations we obtain the following values for k_x, k_y, k_z

$k_x = \frac{m\pi}{L}$, $k_y = \frac{n\pi}{W}$, $k_z = \frac{p\pi}{h}$.

Also $B_1=B_2=B_3=0$.

Therefore the value of

$$A_z = A_1 A_2 A_3 \cos(k_x x')\cos(k_y y')\cos(k_z z') = A_{mnp} \cos(k_x x')\cos(k_y y')\cos(k_z z')$$

Form this value of A_z the field equations are derived as

$$H_x = -\frac{k_y}{\mu} A_{mnp} \cos(k_x x')\sin(k_y y')\cos(k_z z')$$

$$H_y = -\frac{k_x}{\mu} A_{mnp} \sin(k_x x')\cos(k_y y')\cos(k_z z')$$

$$H_z = 0$$

$$E_x = -\frac{j}{\omega\mu\varepsilon} k_x k_z A_{mnp} \sin(k_x x')\cos(k_y y')\sin(k_z z')$$

$$E_y = -\frac{j}{\omega\mu\varepsilon} k_y k_z A_{mnp} \cos(k_x x')\sin(k_y y')\sin(k_z z')$$

$$E_z = -\frac{j(k^2 - k_z^2)}{\omega\mu\varepsilon} A_{mnp} \cos(k_x x')\cos(k_y y')\cos(k_z z')$$

2.2.3 RADIATION EQUATIONS

The fields radiated by the sources **J** and **M** in an unbounded region can be computed by finding the vector potentials **A** and **F** due to **J** and **M** respectively, as follows.

$$\mathbf{A} = \frac{\mu}{4\pi}\iiint_V \mathbf{J}\frac{e^{-jkR}}{R}dv'$$

And

$$\mathbf{F} = \frac{\varepsilon}{4\pi}\iiint_V \mathbf{M}\frac{e^{-jkR}}{R}dv'$$

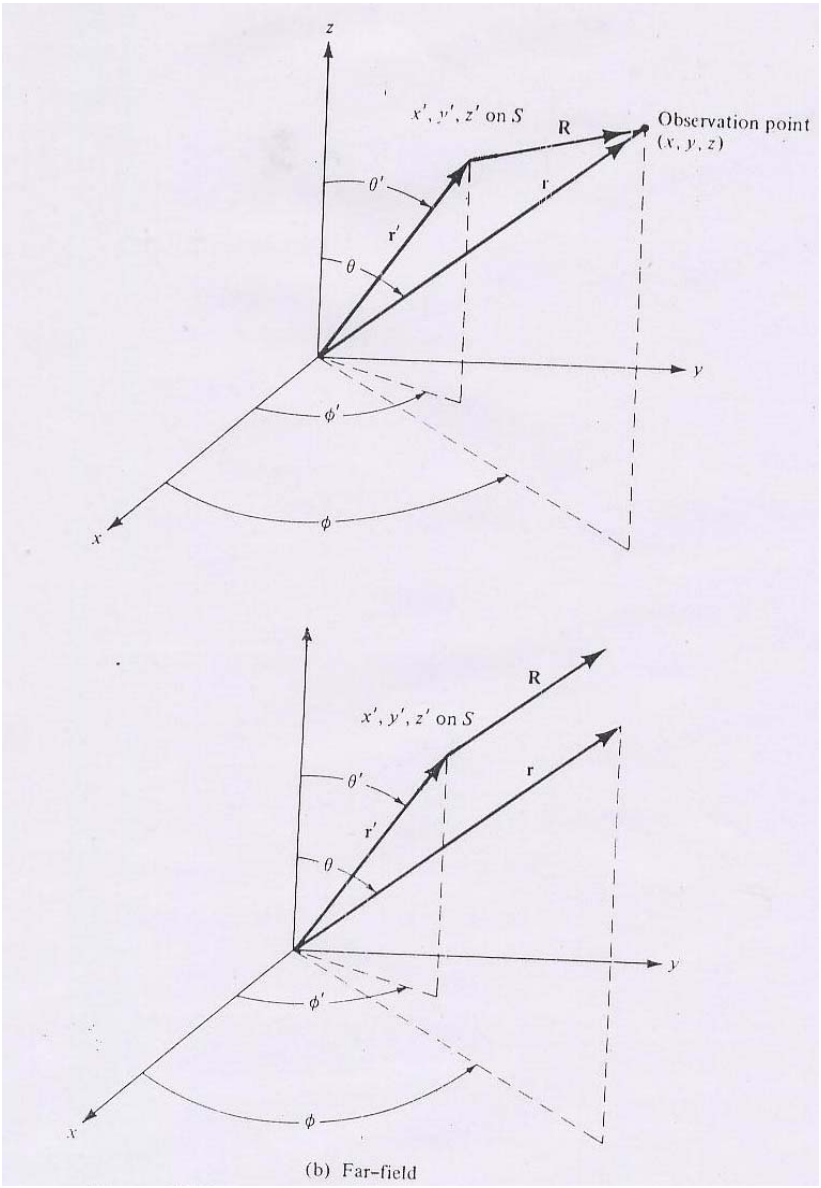

Figure2.5 Coordinate System For Radiation Analysis

The fields radiated by antennas of finite dimensions are spherical waves. For these radiators, a general solution to the vector wave equation $\nabla^2 \mathbf{A_z} + k^2 \mathbf{A_z} = 0$ in spherical components, each as a function of r, θ, φ takes the general form of

$$\mathbf{A} = \mathbf{a}_r A_r(r,\theta,\phi) + \mathbf{a}_\theta A_\theta(r,\theta,\phi) + \mathbf{a}_\phi A_\phi(r,\theta,\phi)$$

The amplitude variations of *r* in each component are of the form $1/r^n$, n = 1, 2. . . Neglecting the higher order terms of $1/r^n$ ($1/r^n = 0$, n = 2,3,. . .),

A reduces to $\mathbf{A} \cong \left[\mathbf{a}_r A_r(r,\theta,\phi) + \mathbf{a}_\theta A_\theta(r,\theta,\phi) + \mathbf{a}_\phi A_\phi(r,\theta,\phi)\right]\dfrac{e^{-jkr}}{r}$, $r \to \infty$

The variations of *r* are separable from the other two components. Neglecting the higher order terms of $1/r^n$, the radiated **E** and **H** fields have only the θ, ϕ components. They can be expressed as

$$\left.\begin{aligned} E_r &\cong 0 \\ E_\theta &\cong -j\omega A_\theta \\ E_\phi &\cong -j\omega A_\phi \end{aligned}\right\} \Rightarrow \mathbf{E_A} = -j\omega\, \mathbf{A}$$

$$\left.\begin{aligned} H_r &\cong 0 \\ H_\theta &\cong +j\frac{\omega}{\eta} A_\phi = -\frac{E_\phi}{\eta} \\ H_\phi &\cong -j\frac{\omega}{\eta} A_\theta = +\frac{E_\theta}{\eta} \end{aligned}\right\} \Rightarrow \mathbf{H_A} = \frac{a_r}{\eta} \times \mathbf{E_A} = -j\frac{\omega}{\eta}\mathbf{a_r} \times \mathbf{A}$$

In a similar manner, the far zone fields due to a magnetic source **M** (potential **F**) can be written as

$$\left.\begin{aligned} H_r &\cong 0 \\ H_\theta &\cong -j\omega F_\theta \\ H_\phi &\cong -j\omega F_\phi \end{aligned}\right\} \Rightarrow \mathbf{H_F} = -\, j\omega\, \mathbf{F}$$

$$\left.\begin{aligned} E_r &\cong 0 \\ E_\theta &\cong -j\omega\eta F_\phi = \eta H_\phi \\ E_\phi &\cong -j\omega\eta F_\theta = -\eta H_\theta \end{aligned}\right\} \Rightarrow \mathbf{E_F} = -\eta\mathbf{a_r} \times \mathbf{H_F} = j\omega\eta\mathbf{a_r} \times \mathbf{F}$$

For far field observations R can most commonly be approximated by

R = $r - r' \cos\psi$ for phase variations

R= r for amplitude variations

Where ψ is the angle between the vectors ***r*** and ***r'*** as shown in the *figure 2.6*

The primed co ordinates (*x', y', z' or r', θ', ϕ'*) indicate the space occupied by the sources $\mathbf{J_s}$ and $\mathbf{M_s}$, over which integration must be performed. The unprimed co ordinates (*x, y, z or r, θ, ϕ*) represent the observation point. Geometrically the vectors **R** and **r** are parallel as shown in the *figure 2.6* below.

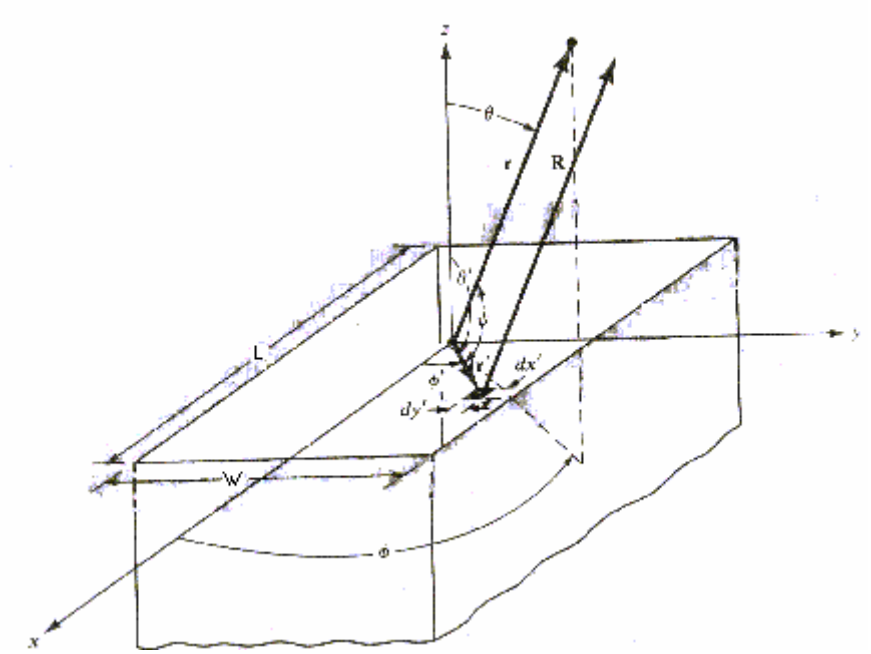

Figure2.6 ***Rectangular Microstrip Patch Antenna Lying on the xy Plane***

The values of **A** and **F** can be calculated as follows

$$\mathbf{A} = \frac{\mu}{4\pi}\iint_S \mathbf{J}_s \frac{e^{-jkR}}{R} ds' \cong \frac{\mu e^{-jkr}}{4\pi r}\mathbf{N}$$

$$\mathbf{N} = \iint_S \mathbf{J}_s e^{jkr'\cos\psi} ds'$$

$$\mathbf{F} = \frac{\varepsilon}{4\pi}\iint_S \mathbf{M}_s \frac{e^{-jkR}}{R} ds' \cong \frac{\varepsilon e^{-jkr}}{4\pi r}\mathbf{L}$$

$$\mathbf{L} = \iint_S \mathbf{M}_s e^{jkr'\cos\psi} ds'$$

As stated, in the far field only the θ and ϕ components of the **E** and **H** fields are dominant. Although the radial components are not necessarily zero, they are negligible compared to θ and ϕ components.

$$(E_A)_\theta \cong -j\omega A_\theta$$
$$(E_A)_\phi \cong -j\omega A_\phi$$

$$(H_F)_\theta \cong -j\omega F_\theta$$
$$(H_F)_\phi \cong -j\omega F_\phi$$

$$(E_F)_\theta \cong +\eta(H_F)_\phi = -j\omega\eta F_\phi$$
$$(E_F)_\phi \cong -\eta(H_F)_\theta = +j\omega\eta F_\theta$$
$$(H_A)_\theta \cong -\frac{(E_A)_\phi}{\eta} = +j\omega\frac{A_\phi}{\eta}$$
$$(H_A)_\phi \cong +\frac{(E_A)_\theta}{\eta} = -j\omega\frac{A_\theta}{\eta}$$

Combining these equations we obtain the total fields in the r, θ and ϕ directions as follows

$$E_r = 0$$
$$E_\theta = \frac{-jke^{-jkr}}{4\pi r}\left(L_\phi + \eta N_\theta\right)$$
$$E_\phi = +\frac{jke^{-jkr}}{4\pi r}\left(L_\theta - \eta N_\phi\right)$$
$$H_r = 0$$
$$H_\theta = \frac{jke^{-jkr}}{4\pi r}\left(N_\phi - \frac{L_\theta}{\eta}\right)$$
$$E_\phi = -\frac{jke^{-jkr}}{4\pi r}\left(N_\theta + \frac{L_\phi}{\eta}\right)$$

Where

$$N_\theta = \iint_S [J_x\cos\theta\cos\phi + J_y\cos\theta\sin\phi - J_z\sin\theta]e^{+jkr'\cos\psi}ds'$$
$$N_\phi = \iint_S [-J_x\sin\phi + J_y\cos\phi]e^{+jkr'\cos\psi}ds'$$
$$L_\theta = \iint_S [M_x\cos\theta\cos\phi + M_y\cos\theta\sin\phi - M_z\sin\theta]e^{+jkr'\cos\psi}ds'$$
$$L_\phi = \iint_S [-M_x\sin\phi + M_y\cos\phi]e^{+jkr'\cos\psi}ds'$$

Considering the patch to be lying in the x-y plane and the radiations are occurring in the z-direction. We therefore have the following configuration

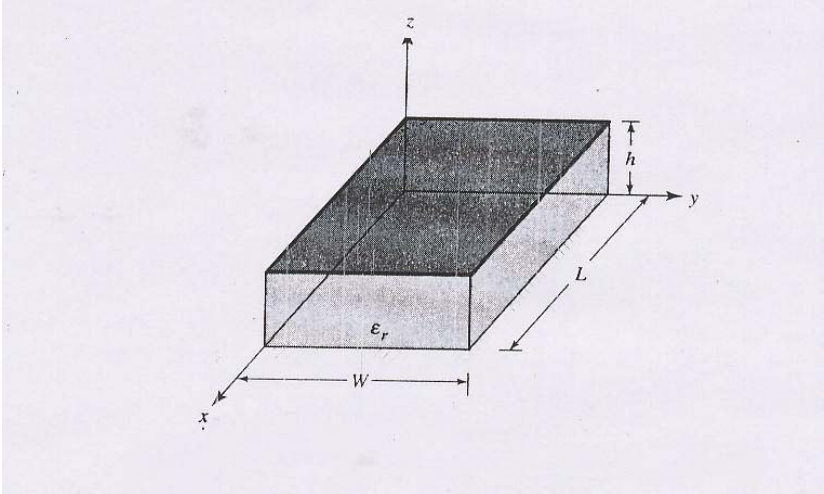

Figure2.7 ***Rectangular Microstrip Patch Geometry***

To reduce the mathematical complexities, initially the field over the opening is assumed to be constant and given by

$$\mathbf{E}_a = \mathbf{a}_y E_0 \qquad -L/2 \le x' \le L/2,\ -W/2 \le y' \le W/2$$

where E_0 is a constant.

To find the fields radiated by this patch, the equivalent is to be formed.

Equivalent

To form the equivalent, closed surface is chosen which extends from - ∞ to + ∞ on the x-y plane.

$$\mathbf{M}_s = -2\mathbf{n} \times \mathbf{E}_a = -2\mathbf{a}_z \times \mathbf{a}_y \mathbf{E}_0 = +\mathbf{a}_x 2\mathbf{E}_0 \qquad -L/2 \le x' \le L/2,\ -W/2 \le y' \le W/2$$

$\mathbf{M}_s = 0$ elsewhere

$\mathbf{J}_s = 0$ everywhere

Radiation Fields: Far Zone and Space Factors

The far zone fields radiated by the slots (cavity modeled microstrip) can be found using the equations described in the previous section.

Thus,

$$L_\theta = \int_{-W/2}^{+W/2} \int_{-L/2}^{+L/2} M_x \cos\theta \cos\phi e^{jk(x'\sin\theta\cos\phi + y'\sin\theta\sin\phi)}\, dx'\, dy'$$

$$= \cos\theta\cos\phi \int_{-W/2}^{+W/2}\int_{-L/2}^{+L/2} M_x e^{jk(x'\sin\theta\cos\phi + y'\sin\theta\sin\phi)}\,dx'\,dy'$$

Using the integral

$$\int_{-c/2}^{+c/2} e^{jaz}\,dz = c\left[\frac{\sin\left(\frac{\alpha}{2}c\right)}{\frac{\alpha}{2}c}\right]$$

$$\therefore L_\theta = 2abE_0\left[\cos\theta\cos\phi\left(\frac{\sin X}{X}\right)\left(\frac{\sin Y}{Y}\right)\right]$$

where
$$X = \frac{kL}{2}\sin\theta\cos\phi$$
$$Y = \frac{kW}{2}\sin\theta\sin\phi$$

Similarly, it can be shown that

$$L_\phi = -2abE_0\left[\sin\phi\left(\frac{\sin X}{X}\right)\left(\frac{\sin Y}{Y}\right)\right]$$

Substituting these values in the field equations we obtain

$$E_r = 0$$
$$E_\theta = j\frac{LWkE_0e^{-jkr}}{2\pi r}\left[\sin\phi\left(\frac{\sin X}{X}\right)\left(\frac{\sin Y}{Y}\right)\right]$$
$$E_\phi = j\frac{LWkE_0e^{-jkr}}{2\pi r}\left[\cos\theta\cos\phi\left(\frac{\sin X}{X}\right)\left(\frac{\sin Y}{Y}\right)\right]$$
$$H_r = 0$$
$$H_\theta = -\frac{E_\phi}{\eta}$$
$$H_\phi = +\frac{E_\theta}{\eta}$$

The total field is the sum of the two-element array with each element representing one of the slots. Since the two slots are identical, this is accomplished by using an array factor for the two slots.

The array factor $(AF)_z = 2\cos\left(\frac{kh}{2}\cos\theta\right)$

Therefore the total electric field in the ϕ direction is

$$E_{\phi}^{t} = j\frac{LWkE_0 e^{-jkr}}{\pi r}\sin\phi\frac{\sin X}{X}\frac{\sin Y}{Y}\cos\left(\frac{kh}{2}\cos\theta\right)$$

3 FEEDING TECHNIQUES

3.1 OVERVIEW

Microstrip antennas have radiating elements on one side of a dielectric substrate, and thus early microstrip antennas were fed either by a microstrip line or a coaxial probe through the ground plane. Since then a number of new feeding techniques have been developed. Prominent among these are coaxial feed, microstrip (coplanar) feed, proximity-coupled microstrip feed, aperture-coupled microstrip feed, and coplanar waveguide (CPW) feed.

Selection of feeding techniques is governed by a number of factors. The most important consideration is the efficient transfer of power between the radiating structure and feed structure, that is, impedance matching between the two. Associated with impedance matching are stepped impedance transformers, bends, stubs, junctions, and so on, which introduce discontinuities leading to spurious radiation and surface wave loss. The undesired radiation may increase the sidelobe level and cross-polar amplitude of the radiation pattern. Minimization of spurious radiation and its effect on the radiation pattern is one of the important factors for evaluation of the feed. Another consideration is the suitability of the feed for array applications. Some feed structures are amenable to better performance because of the larger number of parameters available.

3.2 COAXIAL FEED/PROBE COUPLING

Coupling of power through a probe is one of the basic mechanisms for the transfer of microwave power. The probe can be an inner conductor of a coaxial line in case of coaxial line feeding or it can be used to transfer power from a triplate line (strip line) to a microstrip antenna through a slot in the common ground plane. A typical microstrip antenna using a coaxial connector is shown in figure 3.1.

The coaxial connector is connected to the backside of the printed circuit board, and the coaxial center conductor after passing through the substrate is soldered to the patch metallization. The location of the feed point is determined for the given mode so that the best impedance match is achieved. Excitation of the patch occurs principally through the coupling of the feed current $\mathbf{J_z}$ to the $\mathbf{E_z}$ field of the patch mode.

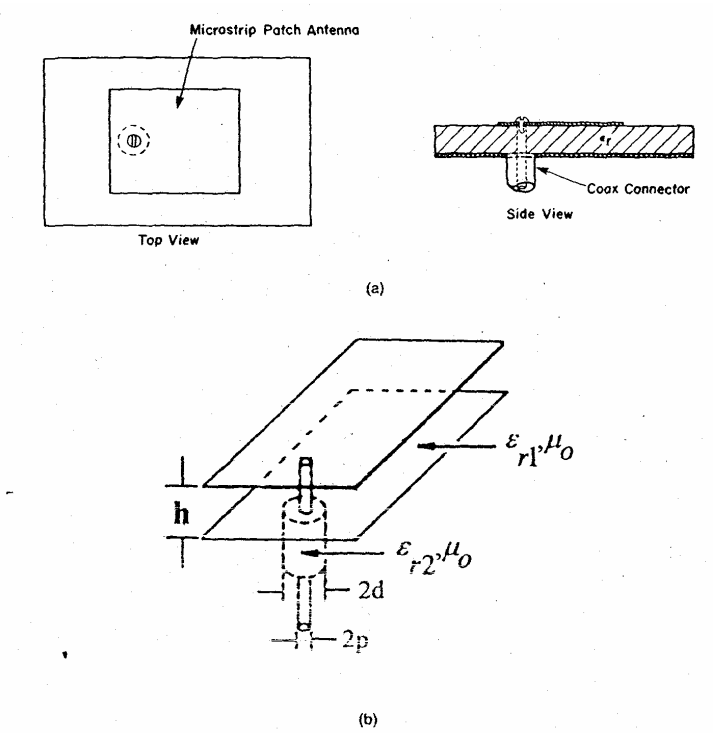

Figure3.1 Coaxial Probe Feeding of a Microstrip Antenna and the Equivalent Circuit for the Probe Junction

3.3 MICROSTRIP FEEDS

Excitation of the microstrip antenna by a microstrip line on the same substrate appears to be natural choice because the patch can be considered an extension of the microstrip line, and both can be fabricated simultaneously, but this technique has some limitations. The coupling between the microstrip line and the patch could be in the form of edge/butt-in coupling as shown in figure 3.2(a*)* or through a gap between them as shown in figure 3.2(b).

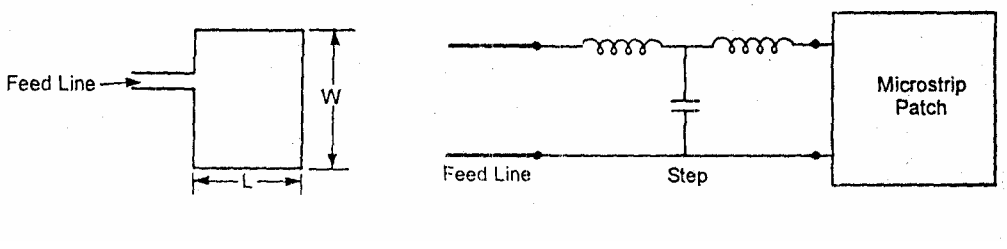

(a) Microstrip Feed at the Radiating Edge

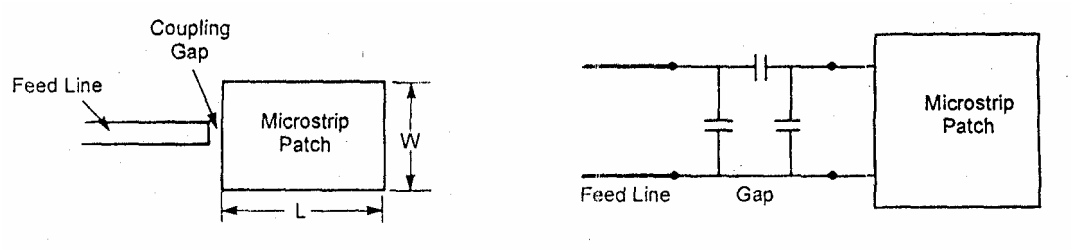

(b) Gap-Coupled Microstrip Feed.

Figure3.2 ***Coplanar Feeds and the Corresponding Equivalent Circuits.***

3.4 PROXIMITY (ELECTROMAGNETICALLY) COUPLED MICROSTRIP FEED

A configuration of this non-contacting microstrip feed is shown in figure 3.3

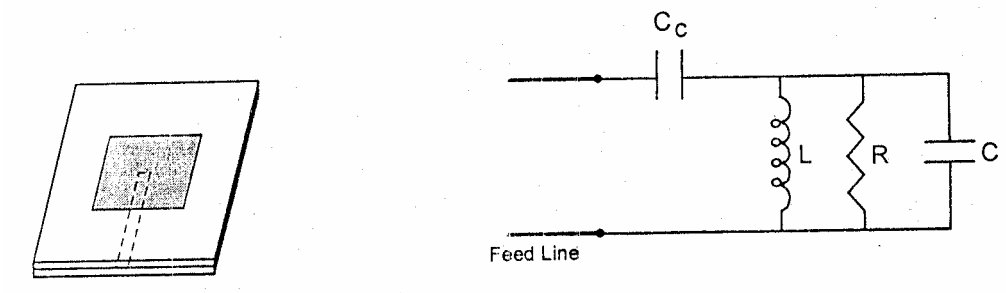

Figure3.3 ***Proximity Coupled Microstrip Feed***

It uses a two-layer substrate with the microstrip line on the lower layer and the patch antenna on the upper layer. The feed line terminates in an open end underneath the patch. This feed is better known as an *electromagnetically coupled* microstrip feed. Coupling between the patch and the microstrip is capacitive in nature. The equivalent circuit for this feed is also shown there, wherein the coupling capacitor C_c is in series with the parallel R-L-C resonant circuit representing the patch. This capacitor can be designed for impedance matching of the antenna, as well as for tuning the patch for improved bandwidth.

The open end of the microstrip line can be terminated in a stub and the stub parameters can be used to improve the bandwidth.

The substrate parameters of the two layers can be selected to increase the bandwidth of the patch, and to reduce spurious radiation from the open end of the microstrip. For this, the lower layer gives a larger bandwidth. Fabrication of this feed is, however, slightly more difficult because of the requirement for accurate alignment between the patch and feed line, but soldering is eliminated.

3.5 APERTURE COUPLED FEED

In this type of feed technique, the radiating patch and the microstrip feed line are separated by the ground plane. Coupling between the patch and feed line is made through a slot or an aperture in a ground plane

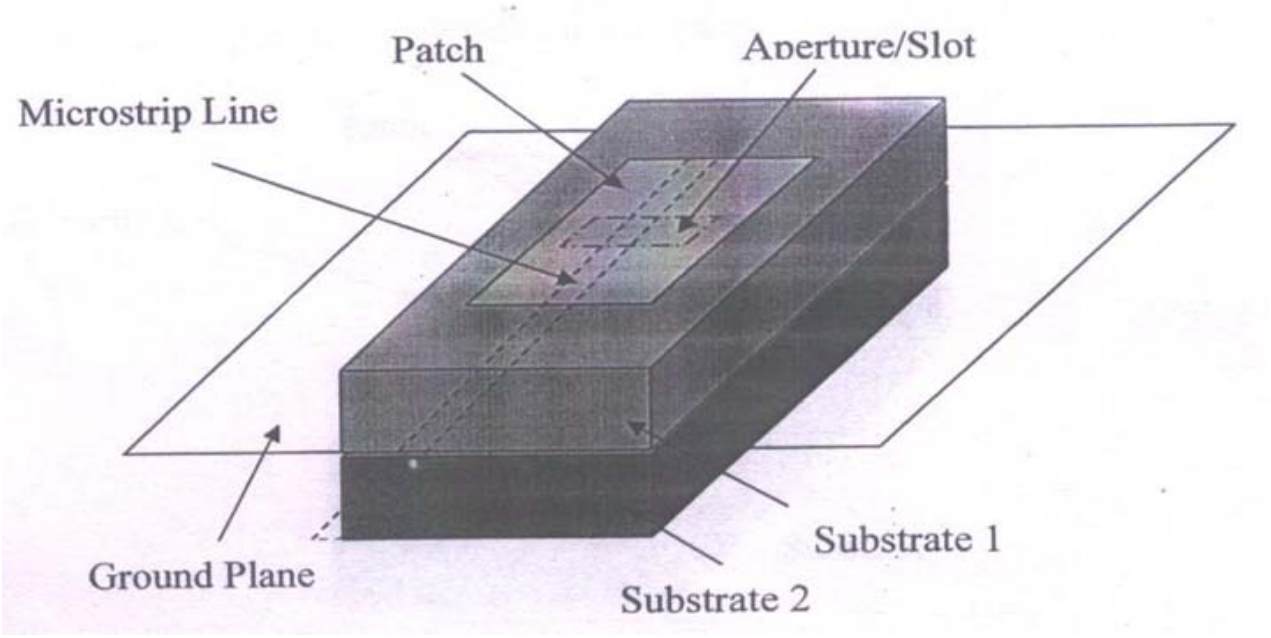

Figure3.4 ***Aperture-coupled Feed***

The coupling aperture is usually centered under the patch, leading to lower cross-polarization due to symmetry of configuration. The shape, size and location of the aperture determine the amount of coupling from the feed line to the patch. Since the ground plane separates the patch and the feed line, spurious radiation is minimized. Generally, a high dielectric material is used for the bottom substrate and a thick, low dielectric constant material is used for the top substrate to optimize radiation from the patch. The major disadvantage of this feed technique is that it is difficult to fabricate due to multiple layers, which also increases the antenna thickness. This feeding scheme also provides narrow bandwidth**.**

The table below summarizes the characteristics of the different techniques.

Characteristics	**Microstrip Line Feed**	**Coaxial Feed**	**Aperture coupled Feed**	**Proximity coupled Feed**
Spurious feed radiation	More	More	Less	Minimum
Ease of fabrication	Easy	Soldering and drilling needed	Alignment required	Alignment required
Impedance matching	Easy	Easy	Easy	Easy
Bandwidth (achieved with impedance matching)	2-5%	2-5%	2-5%	13%
Reliability	Better	Poor due to soldering	Good	Good

.

4 APERTURE-COUPLED MICROSTRIP ANTENNA

4.1 GEOMETRY OF APERTURE COUPLED MICROSTRIP ANTENNAS

Following are the basic elements of aperture-coupled microstrip antennas are:

Radiating Elements:
The original aperture coupled antenna used a single rectangular patch, Since than, researchers demonstrated the use of circular patches, stacked patches, parasitically coupled patches, patches with loading slots, and radiating elements consisting of multiple thin printed dipoles. Most of these modifications are intended to yield improved bandwidth.

Slot Shape:
The shape of coupling aperture has a significant impact on the strength of coupling between the feed line and patch. Thin rectangular coupling slots have been used in the majority of aperture coupled microstrip antennas, as these giving better coupling than round apertures. Slots with enlarged ends bow-tie or H-shaped apertures can further improve coupling.

Type of Feed Line:
The microstrip feed line can be replaced with other planar lines, such as strip line, coplanar waveguide, dielectric waveguide, and similar. The coupling level may be reduced with such lines; however it is also possible to invert the feed substrate, inserting an additional dielectric layer so that the feed line is between the ground plane and the patch element.

Polarization:
Besides linear polarization, it has been demonstrated that dual polarization and circular polarization can be obtained with aperture coupled elements.

Dielectric layers:
As with other type of microstrip antennas, it is very easy to add a random layer to an aperture coupled antenna, either directly over the radiating element, or spaced above the element. It is also possible to form the antenna and feed substrates from multiple layers such as foam with thin dielectric skins for the etched conductors.

4.2 DIMENSIONAL PARAMETERS OF APERTURE COUPLED ANTENNAS

In the aperture coupled microstrip antenna the radiating microstrip patch element is etched on the top of the antenna substrate, and the microstrip feed line is etched on the bottom of the feed substrate. The thickness and dielectric constants of these two substrates may thus be chosen independently to optimize the distinct electrical functions of radiation and circuitry. Although the original prototype antenna used a circular coupling aperture, it was quickly realized that the use of rectangular slot would improve the coupling, for a given aperture area, due to its increased magnetic polarizability. Most aperture-coupled microstrip antennas now use rectangular slots, or variations thereof. The aperture-coupled microstrip antenna involves over a dozen material and dimensional parameters, and the basic trends with variation of these parameters are summarized below:

Antenna substrate dielectric constant:
This primarily affects the bandwidth and the radiation efficiency of the antenna, with lower permittivity giving wider impedance bandwidth and reduced surface wave excitation.

Antenna substrate thickness:
Substrate thickness affects bandwidth and coupling level. A thicker substrate results in wider bandwidth, but less coupling for a given aperture size.

Microstrip patch length:
The length of patch radiator determines resonant frequency of antenna.

Microstrip patch width:
The width of the patch affects the resonant resistance of the antenna, with a wider patch giving the lower resistance. Square patches may result in the generation of high cross polarization levels, and thus should be avoided unless dual or circular polarization is used.

Feed substrate dielectric constant:
This should be selected for good microstrip circuit qualities, typically in the range of 2 to 10.

Feed substrate thickness:
Thinner microstrip substrates result in less spurious radiation from feed lines, but higher loss. A compromise of 0.01λ to 0.02λ is usually good.

Slot length:
The length of the coupling slot, as well as the back radiation level primarily determines the coupling level. The slot should therefore be made no larger than is required for impedance matching.

Slot width:
The width of slot also affects coupling level, but to a much less degree than the slot length. The ratio of a lot length to width is typically 1/10.

Feed line width:
Besides controlling the characteristics impedance of the feed line, the width of the feed line affects the coupling to the slot. To a certain degree, thinner feed lines couple more strongly to the slot.

Feed line position relative to slot:
For maximum coupling the feed line should be positioned at the right angles to the center of the slot. Skewing the feed line from the slot will reduce the coupling, as will positioning the feed line towards the edge of the slot.

Position of the patch relative to the slot:
For maximum coupling, the patch should be centered over the slot. Moving the patch relative to the slot in the H-plane direction has little effect, while moving the patch relative to the slot on the E-plane (resonant) direction will decrease the coupling level.

Length of tuning stub:
The tuning stub is used to tune the excess reactance of the slot coupled antenna. The stub is typically slightly less than $\lambda g/4$ in length; shortening the stub will move the impedance locus in the capacitive direction on the Smith chart (capacitive) on the chart.

4.3 VARIATIONS ON THE APERTURE COUPLED MICROSTRIP ANTENNA

Since the first microstrip antenna was proposed, researchers around the world have suggested a large number of variations in geometry. The fact that the aperture coupled antenna geometry lends itself so well to such modifications is due in part to the nature of printed antenna technology itself, but also to the multi-layer structure of the antenna. Below are some of the modified designs that have evolved from the basic aperture coupled antenna geometry:

Broadband aperture coupled microstrip antennas:
One of the useful features of the microstrip antenna is that it can provide substantially improved impedance bandwidths. While single layer probe or microstrip line-fed elements are typically limited to bandwidth of 2-5 %, aperture coupled elements have been demonstrated with bandwidths up to 10-15% with a single layer and up to 30-50 % with a stacked patch configuration. This improvement in bandwidth is primarily a result of the additional degrees of freedom offered by the stub length and coupling aperture size. The tuning stub length can be adjusted to offset the inductive shift in the impedance that generally occurs when thick antenna substrates are used, and the slot

can be brought close to resonance to achieve a double tuning effect. Se of a stacked patch configuration also introduces a double tuning effect.

Dual and circularly polarized aperture coupled microstrip antennas:
As with other types of microstrip antennas, dual polarization capability can be obtained by using two orthogonal feeds. Circularly polarized aperture coupled elements can also be designed with a single diagonal coupling slot and slightly non square patch similar to circularly polarized patches with a single probe feed, but the resulting axial ratio bandwidth is very narrow. Somewhat improved axial ratio bandwidth can be obtained by using a crossed slot with a single microstrip feed line through the diagonal of the cross, and a slightly non square patch.

Aperture coupled microstrip antenna arrays:
Like other types of microstrip antennas, aperture coupled elements lend themselves well to arrays using either series or corporate feed networks. The two-sided structure of the aperture coupled element allows plenty of space for feed network layout, and this extra room is especially useful for dual polarized or dual frequency arrays. In addition, the ground plane serves as a very effective shield the radiating aperture and feed network. One drawback is that the coupling apertures will radiate a small amount of power in the back direction, but in practice a ground plane located some distance below the feed layer can be used to eliminate this radiation.

5 IE3D SOFTWARE

5.1 OVERVIEW

Electromagnetic simulation is a new technology to yield high accuracy and design of complicated microwave and RF printed circuit, antennas, high speed digital circuits and other electronic components. IE3D is an integrated full-wave electromagnetic simulation and optimization package for the analysis and design of 3-dimensional microstrip antennas and high frequency printed circuits and digital circuits, such as microwave and millimeter-wave integrated circuits (MMICs) and high speed printed circuit boards (PCBs). The IE3D has been adopted as an industrial standard in planar and 3D electromagnetic simulation. It has become the most versatile, easy to use, efficient and accurate electromagnetic simulation tool.

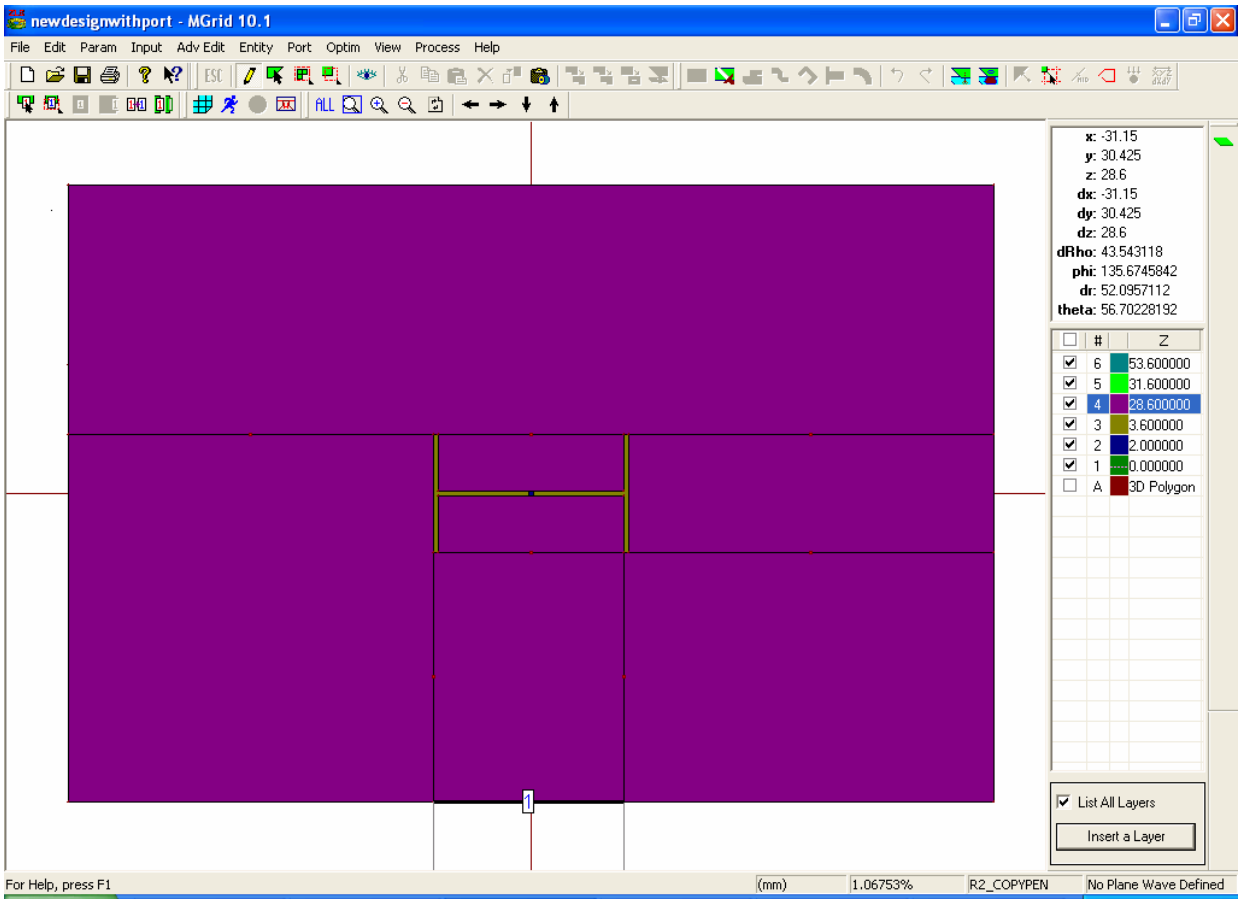

Figure5.1 The Design Window of IE3D

IE3D application programs and capability:

The IE3D package consists of the following major application programs:

- **MGRID**

  Layout editor for the construction of a geometry, and post processor for current display and pattern calculation

- **IE3D**

  Electromagnetic simulator or simulation engine for numerical analysis.

- **MODUA**

  Schematic editor for parameter display and nodal circuit simulation.

- **PATTERNVIEW**

  Post processor for radiation patterns.

- **IE3DLIBRARY**

  The object oriented 2nd IE3D interface for parameterized geometry construction.

- **CURVIEW**

  Post processor for display of current distribution and field distribution.

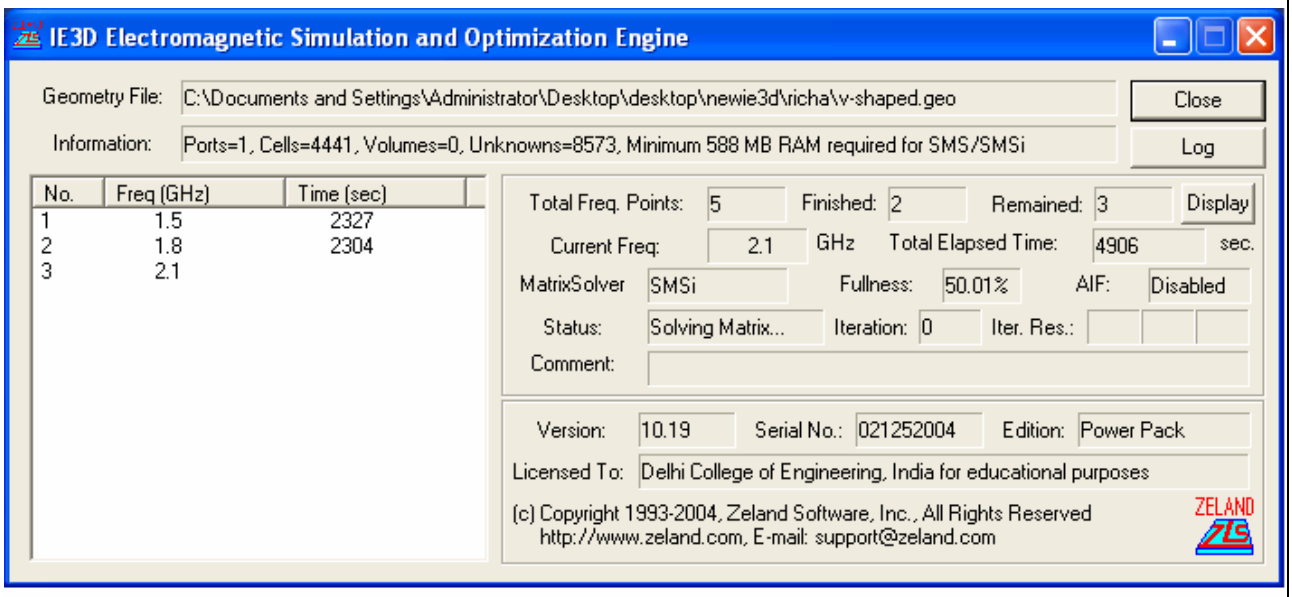

Figure5.2 ***The Simulation Window of IE3D***

One of the major advantages of electromagnetic simulation is that field and current distributions from a simulated structure are accessible to the users. Information on the current and field distribution can be valuable to circuit and antenna designers. It allows comparison of radiation patterns from different frequencies of the same structure or different structures. The IE3D has a great advantage over other

commercial electromagnetic simulation tools no matter whether accuracy, efficiency, capability or usability is concerned.

5.2 STANDARD SYNTHESIS FORMULAE (Z_0, ε_r, h, f_0 given)

Various workers have reported formulae for microstrip calculations. Owens carefully investigated the ranges of applicability of many of the expressions given by Wheeler, comparing calculated results with numerical computations requiring elaborate algorithms-but known to be very accurate. New changeover values for the shape ratio (w/h) were advocated for greatest accuracy by using alternate expressions dependent upon w/h range. For narrow strips (i.e. when $Z_0 > \{44\text{-}2\ \varepsilon_r\}$)

$$\frac{w}{h} = \left(\frac{\exp H'}{8} - \frac{1}{4 \exp H'} \right)^{-1}$$

$$H' = \frac{Z_0 \sqrt{2\varepsilon_r + 2}}{119.9} + \frac{1}{2}\left(\frac{\varepsilon_r - 1}{\varepsilon_r + 1} \right)\left(\ln \frac{\pi}{2} + \frac{1}{\varepsilon_r} \ln \frac{4}{\pi} \right)$$

$$\varepsilon_{eff} = \frac{\varepsilon_r + 1}{2}\left\{ 1 - \frac{1}{2H'}\left(\frac{\varepsilon_r - 1}{\varepsilon_r + 1} \right)\left(\ln \frac{\pi}{2} + \frac{1}{\varepsilon_r} \ln \frac{4}{\pi} \right) \right\}^{-2}$$

The value of ε_{eff} is not independent of frequency. The frequency dependent value is given by

$$\varepsilon_{eff}(f) = \varepsilon_r - \frac{\varepsilon_r - \varepsilon_{eff}}{1 + (h/Z_0)^{1.33}(0.43 f^2 - 0.009 f^3)}$$

The length of the patch L is given by $L = \lambda / 2$ where λ is the free space wavelength.

Because of fringing effects, electrically the patch of the microstrip antenna looks greater than its physical dimensions. For the principal E-plane (xy plane), this is shown in

figure 4.2. where dimensions of the patch have been extended on each end by a

distance ΔL.

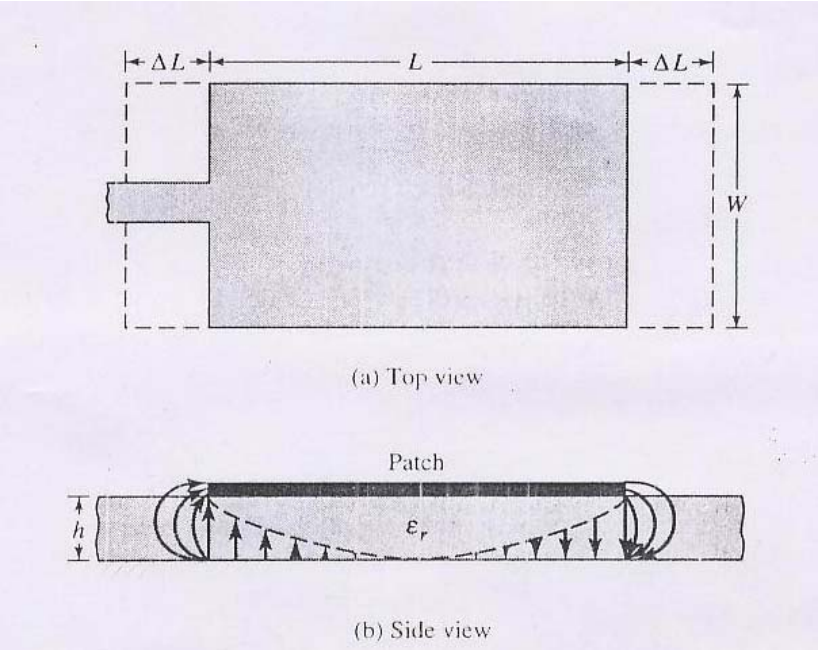

Figure5.3 Physical and Effective Lengths of Rectangular Microstrip Patch

$$\frac{\Delta L}{h} = 0.412 \frac{\left(\varepsilon_{eff} + 0.33\right)\left(\frac{W}{h} + 0.264\right)}{\left(\varepsilon_{eff} - 0.258\right)\left(\frac{W}{h} + 0.8\right)}$$

The effective length of the patch $L_e = L + 2\ \Delta L$.

The resonant frequency of the microstrip patch is given by

$$f_r = \frac{c}{2L_e\sqrt{\varepsilon_{eff}}}$$

6 DESIGN OF BROADBAND DUAL-FREQUENCY MICROSTRIP ANTENNA

6.1 INTRODUCTION

Broadband Dual-Frequency Microstrip Antenna can be implemented by any of the two methods, one with a two element radiating patch and one using a three-dimensional V-shaped radiating. These designs are suitable for base station antennas for wireless communications systems. Broadband dual-frequency operation can be obtained by the use of (a) two aperture-coupled feeds, (b) a gap coupled probe feed and an H-slot coupled feed and (c) an L-strip coupled feed and an H-slot coupled feed.

6.2 DESIGN OF A THREE-DIMENSIONAL V-SHAPED MICROSTRIP ANTENNA

In this design broadband dual-frequency operation has been demonstrated with the use of a V-shaped radiating patch. Figure 6.1 shows the geometry of a broadband dual frequency V-shaped microstrip patch antenna.

The V-shaped patch has dimensions L X W, and the patch's centerline (AB) and nonradiating edges are, respectively, distances h_1 and h_2 from the ground plane; h_1 is usually selected to be small, about $0.02\lambda_0$ (λ_0 is the free space operating frequency) such that smaller coupling slot can be used for achieving efficient coupling of the electromagnetic energy from the microstrip line to the radiating V-shaped patch. The distance h_2 is chosen to be much greater h_1, which effectively increases antenna's average substrate thickness and makes possible the excitation of broadband resonant modes. An H-shaped coupling slot is cut in the ground plane of the microstrip line and centered below the V-shaped patch.

The use of an H-shaped slot allows a smaller slot size for efficient electromagnetic energy coupling and thus the reduction in the back radiation in the slot. The H-shaped slot is narrow, 1 mm wide. The lengths of the slot's central arm and two side arms are H_1 and H_2, respectively; both are much greater than 1 mm. The microstrip line has line has a width w_f and tuning–stub length t, and is designed to have a 50 Ω characteristic impedance.

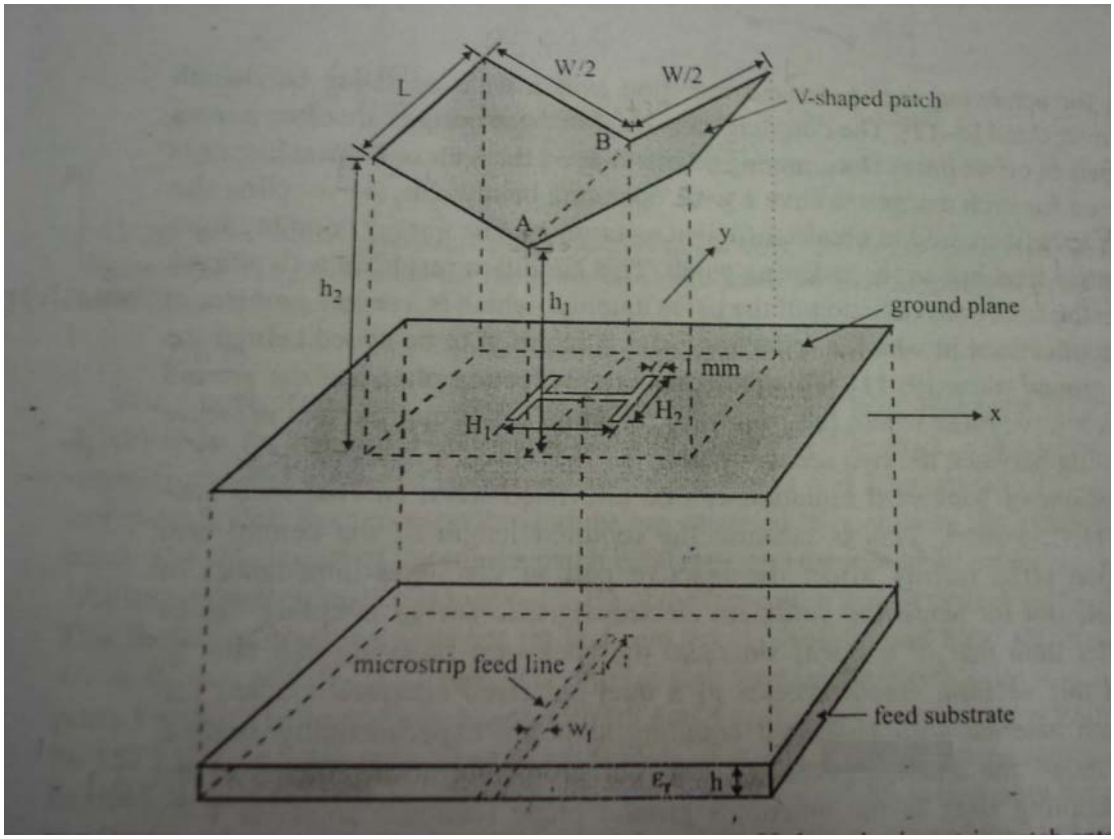

Figure6.1 Geometry of ***V Shaped Microstrip Patch Antenna***

6.3 FEEDING TECHNIQUE USED IN THIS DESIGN

Selection of feeding techniques is governed by a number of factors. The most important being efficient transfer of power between the radiating structure and feed structure i.e. impedance matching between the two. Minimization of spurious radiation and its effect on the radiation pattern is one of the important factors for evaluation of feed.

The feeding technique used here is the **Microstrip Feed Line**. In this type of feed technique, a conducting strip is connected directly to the edge of the Microstrip patch. The conducting strip is smaller in width as compared to the patch and this kind of feed arrangement has the advantage that the feed can be etched on the same substrate to provide a planar structure.

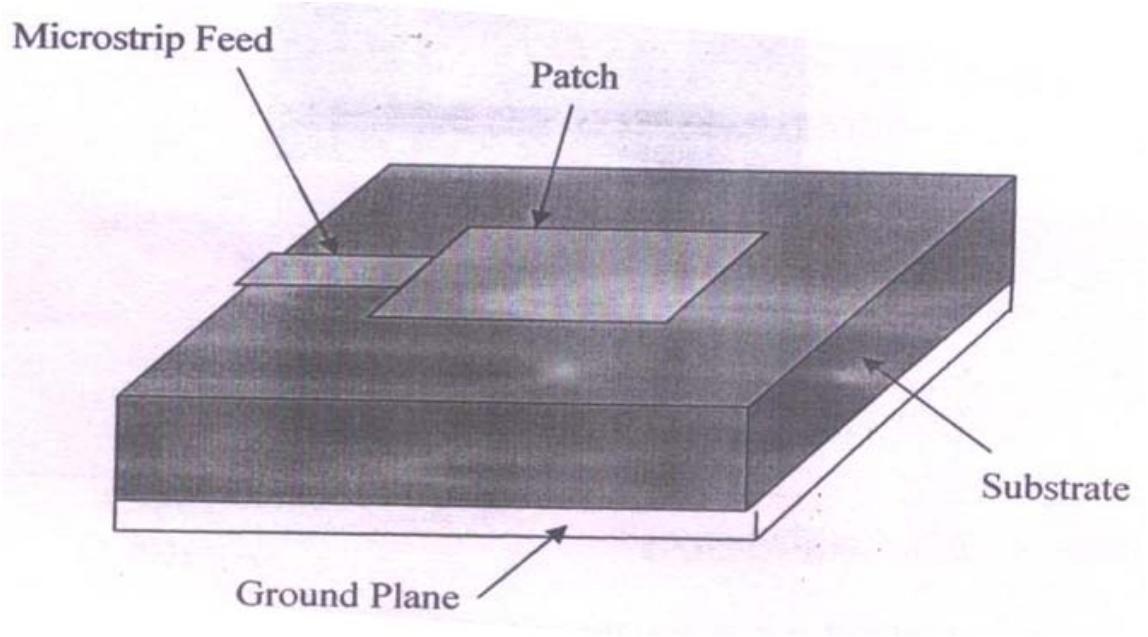

Figure6.2 ***Microstrip Line Feed***

The purpose of the inset cut in the patch is to match the impedance of the feed line to the patch without for any additional matching element. This is achieved by properly controlling the inset position. Hence this is an easy feeding scheme, since it provides ease of fabrication and simplicity in modeling as well as impedance matching. However as the thickness of the dielectric substrate being used, increases, surface waves and spurious feed radiation also increases, which hampers the bandwidth of the antenna. The feed radiation also leads to undesired cross polarized radiation.

6.4 DESIGN OF A BROADBAND V-SHAPED MICROSTRIP PATCH RADIATOR

A V-shaped microstrip antenna has been designed for the following specifications,

L = 60 mm	$\varepsilon_r = 4.4$
W = 105 mm	h = 1.6 mm
$H_1 = 37$ mm	$h_1 = 3$ mm
$H_2 = 23$ mm	t = 25 mm

Ground plane size; length = 180 mm, width = 120 mm.

This antenna is modeled using IE3D software. Three dimensional view of designed antenna is shown below:

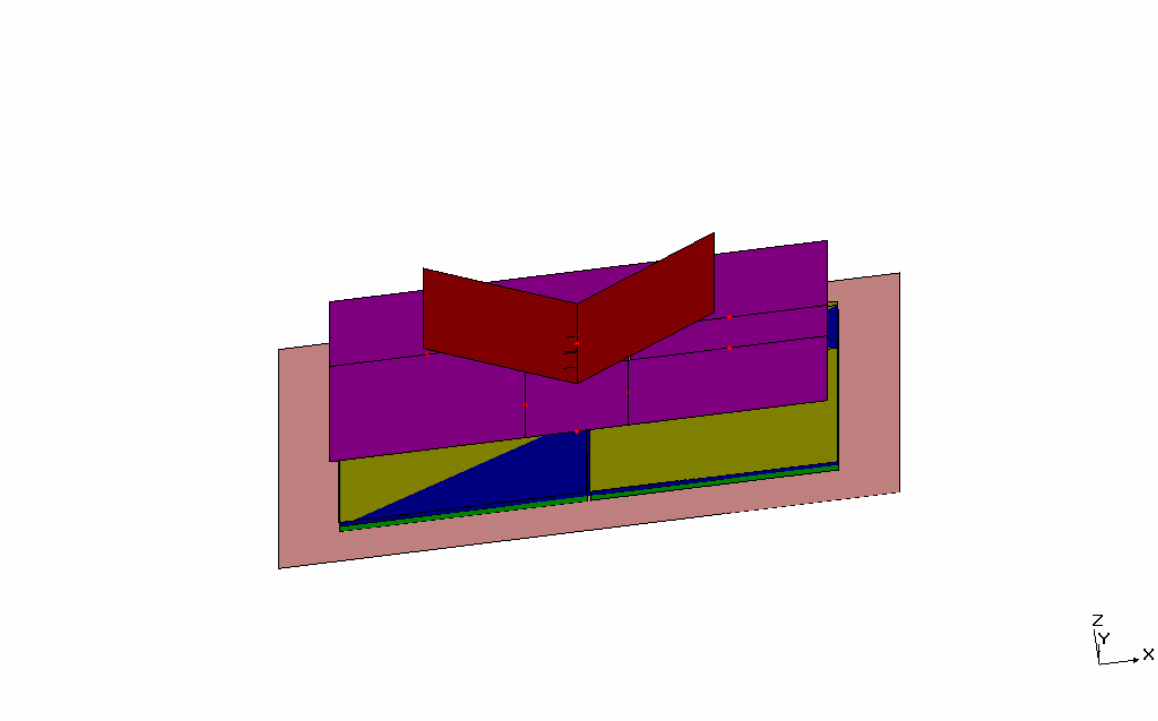

Figure6.3 ***Three - dimensional view of designed antenna***

7 RESULTS OF SIMULATION OF THE MICROSTRIP ANTENNA DESIGN

7.1 THE S-PARAMETER PLOT

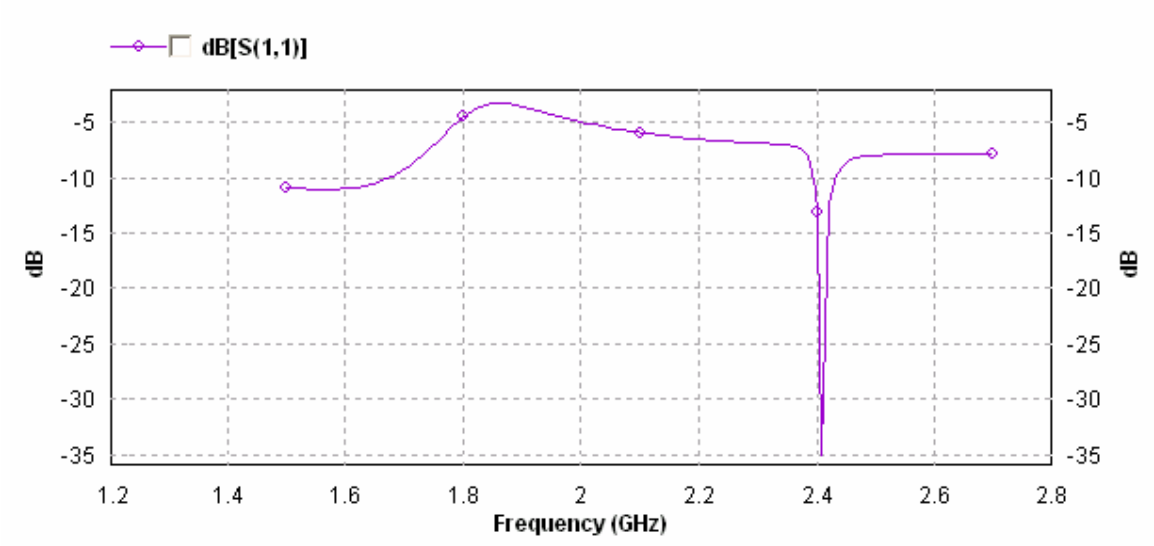

Figure7.1 ***The S_{11} (dB) Plot for the Microstrip Antenna***

7.2 RADIATION PATTERN

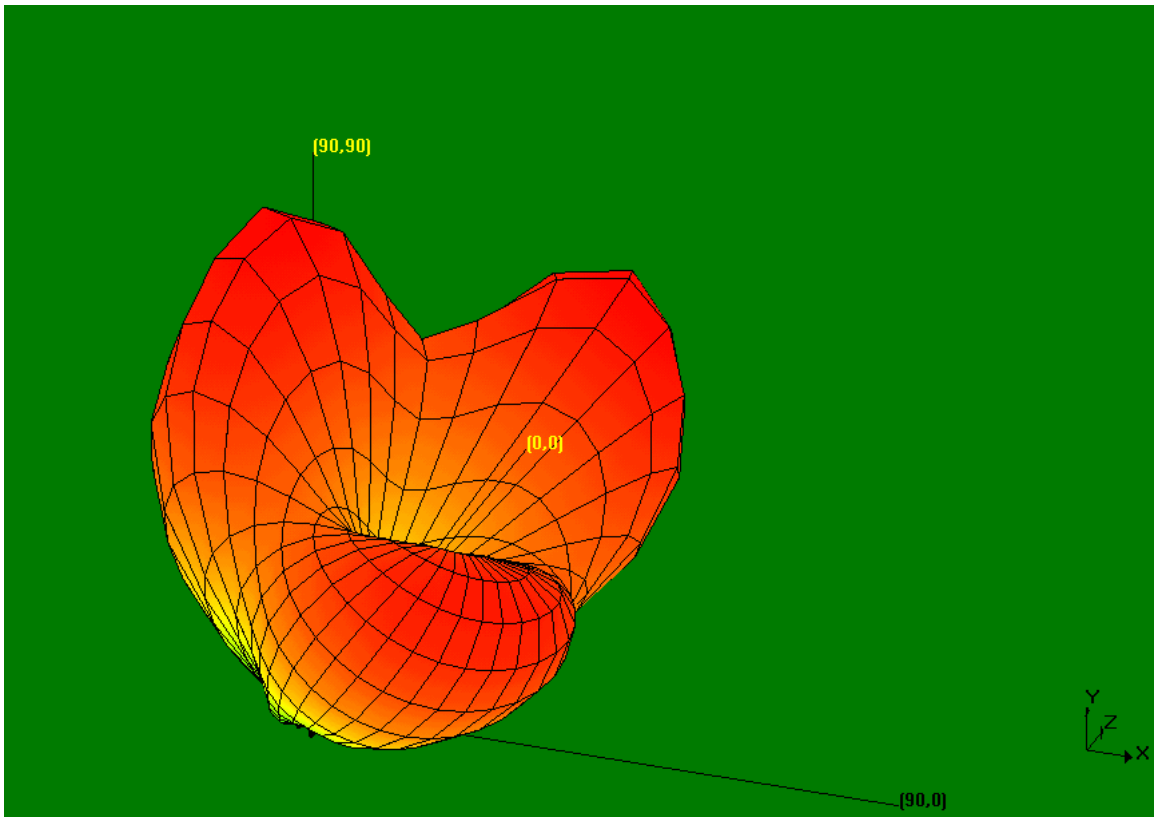

Figure7.2 ***Radiation Pattern of the Simulated Microstrip Antenna***

Another view of radiation pattern of the designed antenna;

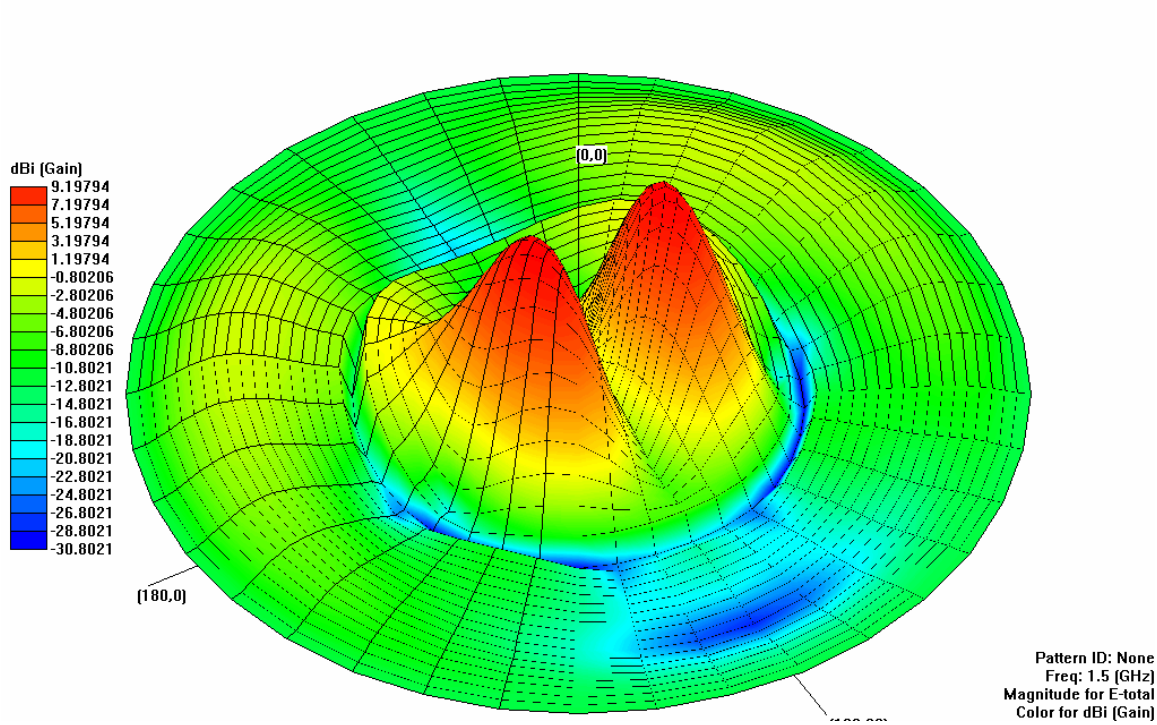

Figure7.3 ***Radiation Pattern of the Simulated Microstrip Antenna (mapped 3d view)***

7.3 ELEVATION PATTERN

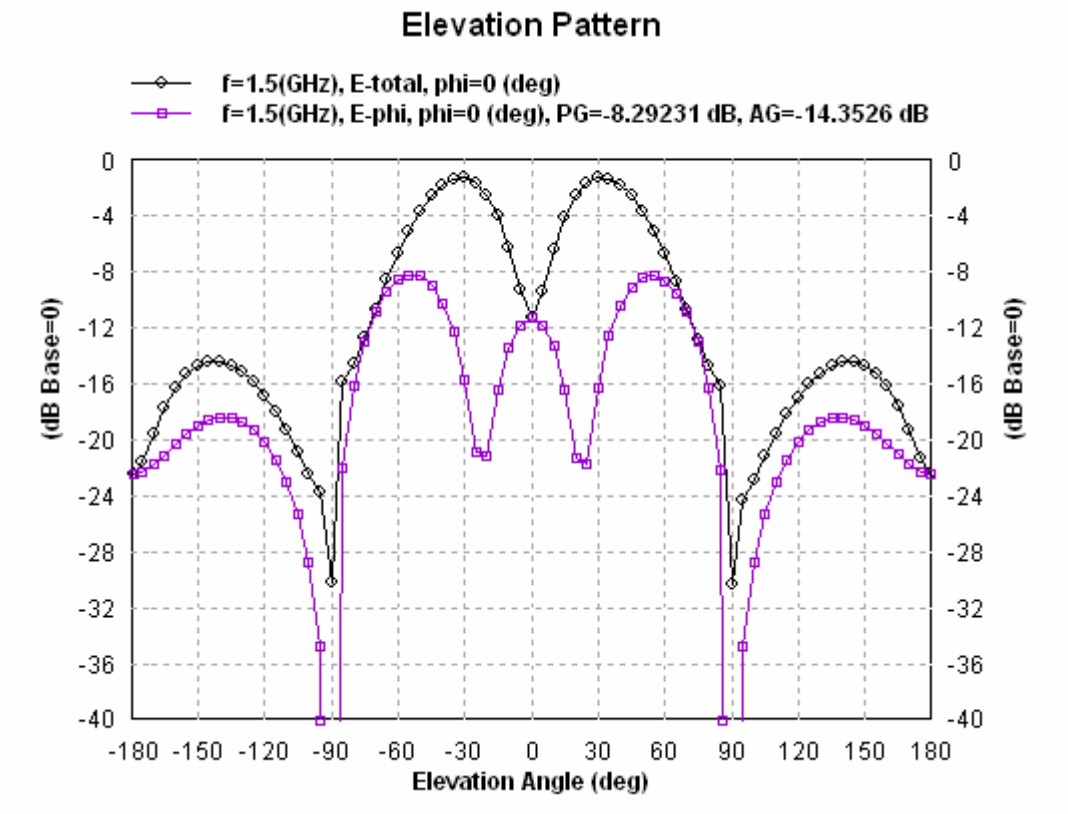

Figure7.4 ***Elevation Pattern Gain Display of the Simulated Microstrip Antenna***

7.4 DIRECTIVITY PLOT

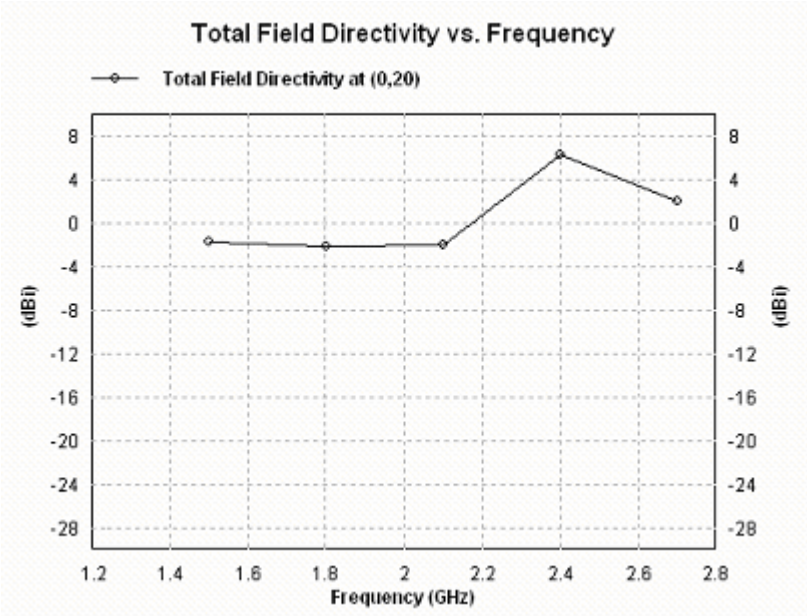

Figure7.5 ***Directivity vs. Frequency plot for the simulated antenna***

7.5 TOTAL FIELD GAIN

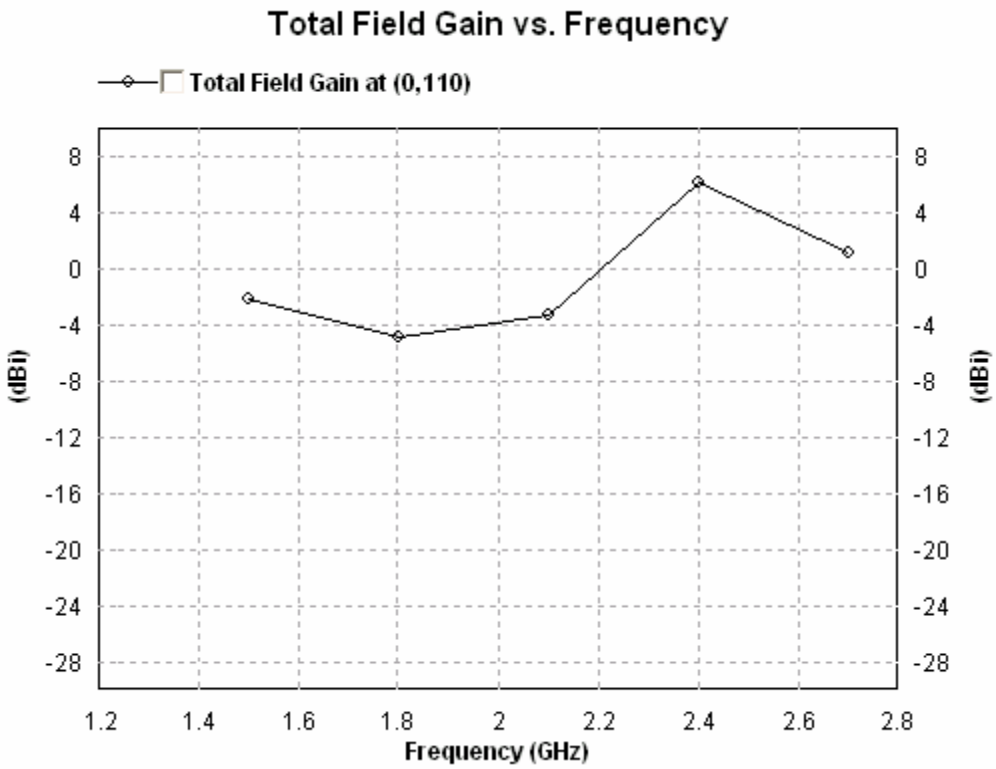

*Figure7.6 T**otal Field Gain vs. Frequency plot for the simulated microstrip antenna***

7.6 ANTENNA AND RADIATION EFFICIENCY

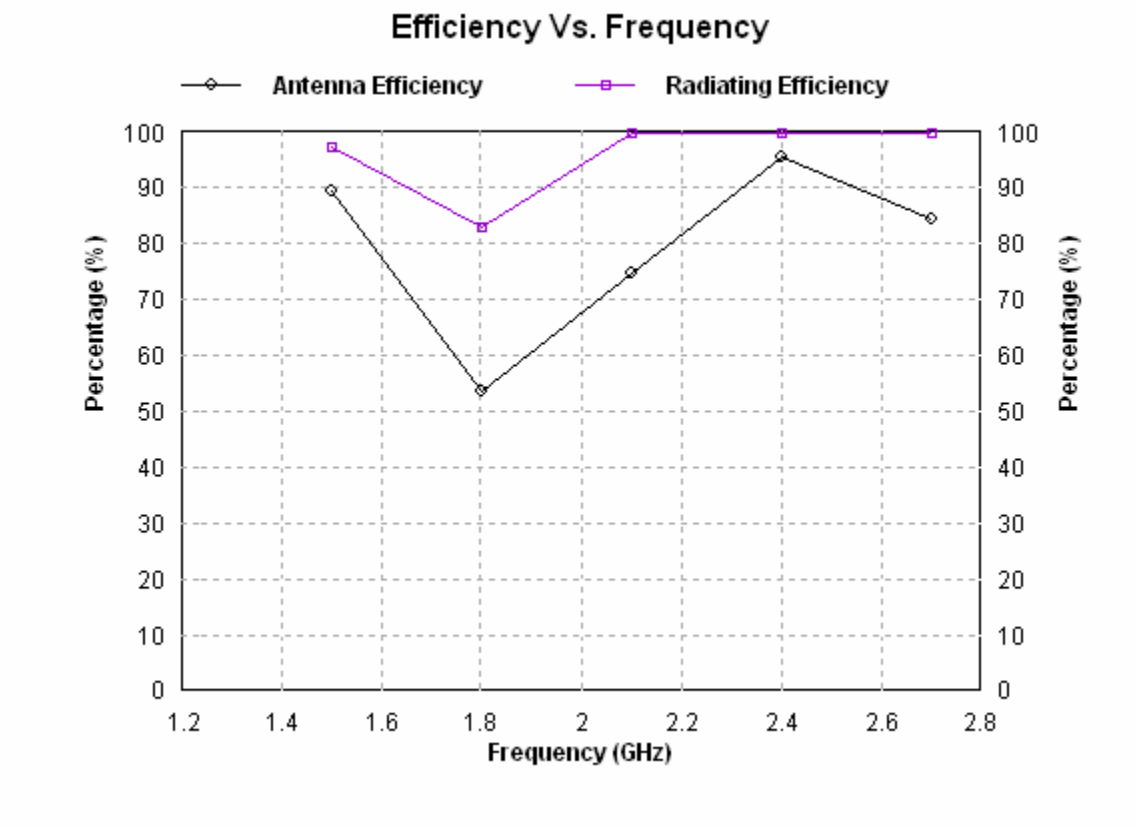

Figure7.7 ***Efficiency Vs. Frequency Plot of the Simulated Antenna***

7.7 AXIAL RATIO

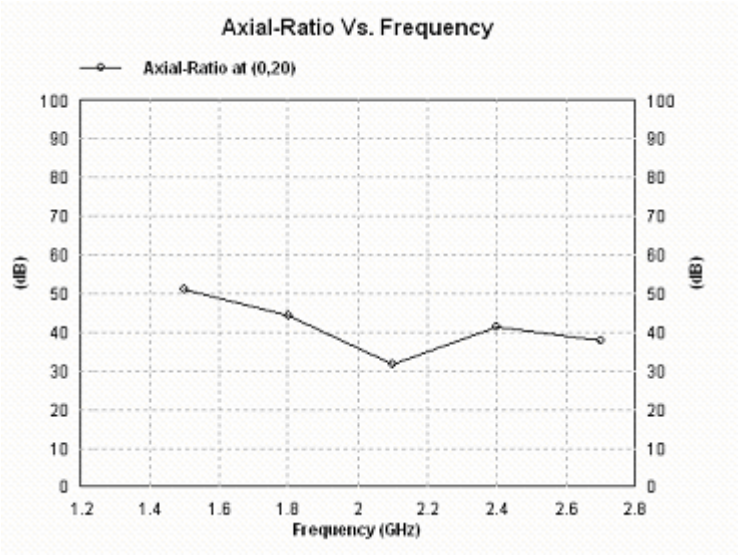

Figure7.8 ***Axial Ratio Vs. Frequency Plot of the Simulated Antenna***

7.8 IMPEDANCE

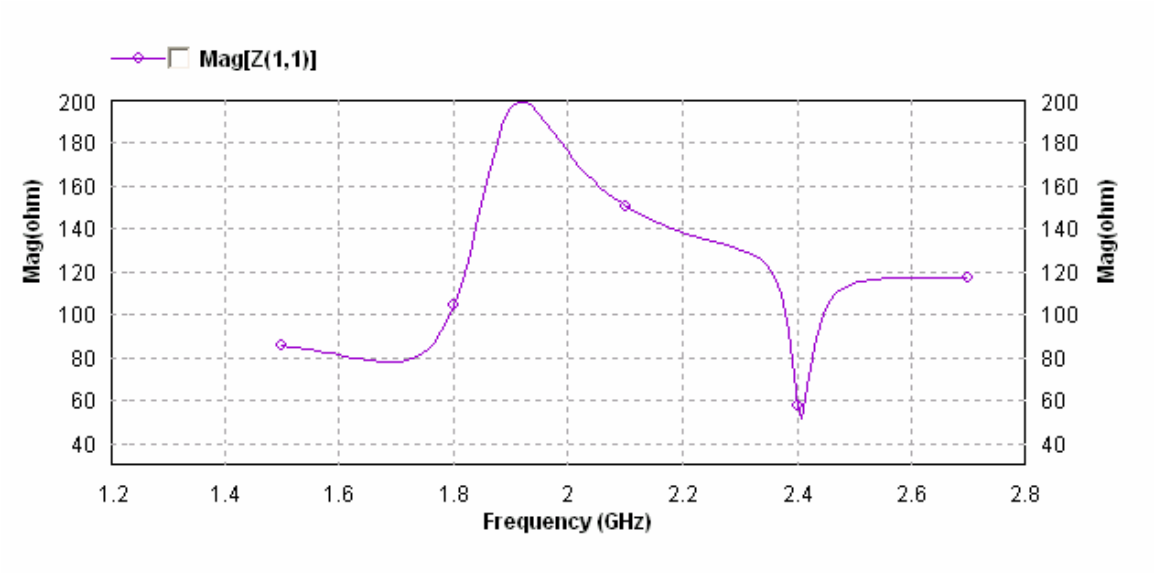

Figure7.9 ***Impedance Vs. Frequency Plot of the Simulated Antenna***

7.9 FREQUENCY PROPERTY

File Name	C:\Documents and Settings\Administrator\Desktop\desktop\newie3d\richa\newdesignwithport.pat
Pattern ID	
Port Number	1
Frequency	1.5 (GHz)
Incident Power	0.01 (W)
Input Power	0.00919679 (W)
Radiated Power	0.00891214 (W)
Average Radiated Power	0.000709206 (W/s)
Radiation Efficiency	96.905%
Antenna Efficiency	89.1214%
Total Field Properties	
Gain	9.19794 dBi
Directivity	9.69812 dBi
Maximum	at (35, 150) deg.

3dB Beam Width	(34.1283, 51.0285) deg.
Theta Field Properties	
Gain	8.72795 dBi
Directivity	9.22813 dBi
Maximum	at (35, 160) deg.
3dB Beam Width	(27.8447, 38.7195) deg.
Phi Field Properties	
Gain	6.63141 dBi
Directivity	7.13159 dBi
Maximum	at (40, 50) deg.
3dB Beam Width	(24.3648, 45.3026) deg.
Left-Hand Circular Field Properties	
Gain	7.18007 dBi
Directivity	7.68025 dBi
Maximum	at (35, 140) deg.
3dB Beam Width	(34.453, 48.7686) deg.

Right-Hand Circular Field Properties	
Gain	7.07658 dBi
Directivity	7.57676 dBi
Maximum	at (35, 40) deg.
3dB Beam Width	(34.3907, 48.726) deg.
No. 1 Port	Inc=1/0 (V), Zs=(50,0) Ohms, Zc=(50,0) Ohm
	V=1.26955/4.45261 (V), I=0.0148173/-7.645 (A)
	Inc=1/1.59028e-014 (V), Ref=0.28341/20.3508 (V)
Frequency	1.8 (GHz)
Incident Power	0.01 (W)
Input Power	0.00647355 (W)
Radiated Power	0.00534367 (W)
Average Radiated Power	0.000425236 (W/s)
Radiation Efficiency	82.5463%
Antenna Efficiency	53.4367%
Total Field Properties	
Gain	5.30164 dBi

Directivity	8.02324 dBi
Maximum	at (45, 170) deg.
3dB Beam Width	(34.5465, 64.0084) deg.
Theta Field Properties	
Gain	4.92804 dBi
Directivity	7.64964 dBi
Maximum	At (40, 140) deg.
3dB Beam Width	(27.4336, 31.3704) deg.
Phi Field Properties	
Gain	5.05729 dBi
Directivity	7.77889 dBi
Maximum	At (50, 180) deg.
3dB Beam Width	(28.315, 38.0938) deg.
Left-Hand Circular Field Properties	
Gain	2.71658 dBi
Directivity	5.43818 dBi

Maximum	at (40, 20) deg.
3dB Beam Width	(33.391, 53.2316) deg.
Right-Hand Circular Field Properties	
Gain	2.70987 dBi
Directivity	5.43147 dBi
Maximum	at (40, 160) deg.
3dB Beam Width	(33.3308, 53.3934) deg.
No. 1 Port	Inc=1/0 (V), Zs=(50,0) Ohms, Zc=(50,0) Ohm
	V=1.48324/16.292 (V), I=0.0142166/-35.8291 (A)
	Inc=1/9.38264e-014 (V), Ref=0.59384/44.4826 (V)
Frequency	2.1 (GHz)
Incident Power	0.01 (W)
Input Power	0.00745944 (W)
Radiated Power	0.00745944 (W)
Average Radiated Power	0.000593603 (W/s)
Radiation Efficiency	100%

Antenna Efficiency	74.5944%
Total Field Properties	
Gain	7.17027 dBi
Directivity	8.44321 dBi
Maximum	at (35, 90) deg.
3dB Beam Width	(34.5073, 67.0069) deg.
Theta Field Properties	
Gain	7.17015 dBi
Directivity	8.44309 dBi
Maximum	at (35, 90) deg.
3dB Beam Width	(34.3964, 48.7528) deg.
Phi Field Properties	
Gain	4.18277 dBi
Directivity	5.45571 dBi
Maximum	at (35, 310) deg.
3dB Beam Width	(25.6805, 40.683) deg.

Left-Hand Circular Field Properties	
Gain	4.91876 dBi
Directivity	6.1917 dBi
Maximum	at (35, 110) deg.
3dB Beam Width	(35.4063, 93.7966) deg.
Right-Hand Circular Field Properties	
Gain	4.90126 dBi
Directivity	6.1742 dBi
Maximum	at (35, 60) deg.
3dB Beam Width	(35.8666, 95.7715) deg.
No. 1 Port	Inc=1/0 (V), Zs=(50,0) Ohms, Zc=(50,0) Ohm
	V=1.50303/1.48939 (V), I=0.00998016/-4.49018 (A)
	Inc=1/-6.75868e-015 (V), Ref=0.50404/4.44526 (V)
Frequency	2.4 (GHz)
Incident Power	0.01 (W)
Input Power	0.00951348 (W)

Radiated Power	0.00951348 (W)
Average Radiated Power	0.000757059 (W/s)
Radiation Efficiency	100%
Antenna Efficiency	95.1348%
Total Field Properties	
Gain	7.79842 dBi
Directivity	8.01503 dBi
Maximum	at (40, 120) deg.
3dB Beam Width	(39.8321, 98.3943) deg.
Theta Field Properties	
Gain	7.34525 dBi
Directivity	7.56186 dBi
Maximum	at (15, 270) deg.
3dB Beam Width	(23.5924, 30.4012) deg.
Phi Field Properties	
Gain	6.05994 dBi

Directivity	6.27655 dBi
Maximum	at (0, 0) deg.
3dB Beam Width	(5.00089, 86.8551) deg.
Left-Hand Circular Field Properties	
Gain	7.6113 dBi
Directivity	7.8279 dBi
Maximum	at (45, 120) deg.
3dB Beam Width	(36.7102, 83.3153) deg.
Right-Hand Circular Field Properties	
Gain	7.58313 dBi
Directivity	7.79973 dBi
Maximum	at (45, 60) deg.
3dB Beam Width	(36.1481, 83.3092) deg.
No. 1 Port	Inc=1/0 (V), Zs=(50,0) Ohms, Zc=(50,0) Ohm
	V=1.09494/10.9178 (V), I=0.0189568/-12.6383 (A)
	Inc=1/-5.56597e-015 (V), Ref=0.220571/70.0871 (V)

Frequency	2.7 (GHz)
Incident Power	0.01 (W)
Input Power	0.00839358 (W)
Radiated Power	0.00839358 (W)
Average Radiated Power	0.00066794 (W/s)
Radiation Efficiency	100%
Antenna Efficiency	83.9358%
Total Field Properties	
Gain	8.19865 dBi
Directivity	8.95918 dBi
Maximum	at (40, 140) deg.
3dB Beam Width	(40.1613, 54.4142) deg.
Theta Field Properties	
Gain	5.52922 dBi
Directivity	6.28975 dBi
Maximum	at (45, 50) deg.
3dB Beam Width	(33.4356, 86.2768) deg.

Phi Field Properties	
Gain	6.40384 dBi
Directivity	7.16437 dBi
Maximum	at (35, 150) deg.
3dB Beam Width	(27.0023, 46.1547) deg.
Left-Hand Circular Field Properties	
Gain	7.98129 dBi
Directivity	8.74182 dBi
Maximum	at (40, 140) deg.
3dB Beam Width	(38.7002, 53.9894) deg.
Right-Hand Circular Field Properties	
Gain	7.93474 dBi
Directivity	8.69526 dBi
Maximum	at (40, 40) deg.
3dB Beam Width	(38.5649, 54.401) deg.

No. 1 Port	Inc=1/0 (V), Zs=(50,0) Ohms, Zc=(50,0) Ohm
	V=1.40056/-0.670073 (V), I=0.0119951/1.56492 (A)
	Inc=1/6.95746e-016 (V), Ref=0.400802/-2.3421 (V)

7.10 RADIATION PATTERN OF MODIFIED DESIGN

When the angle of V-shaped patch is decreased then we get radiation pattern as shown below.

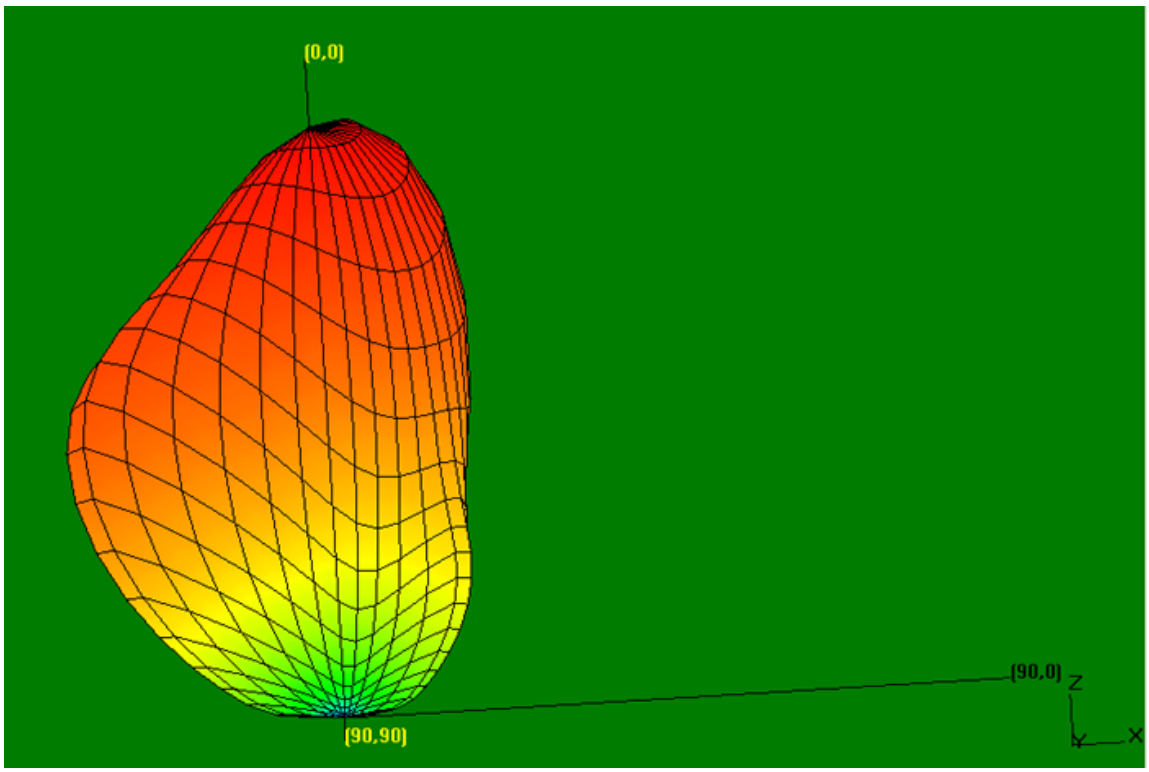

Figure7.10 Radiation Pattern of the Simulated Microstrip Antenna with decreased angle

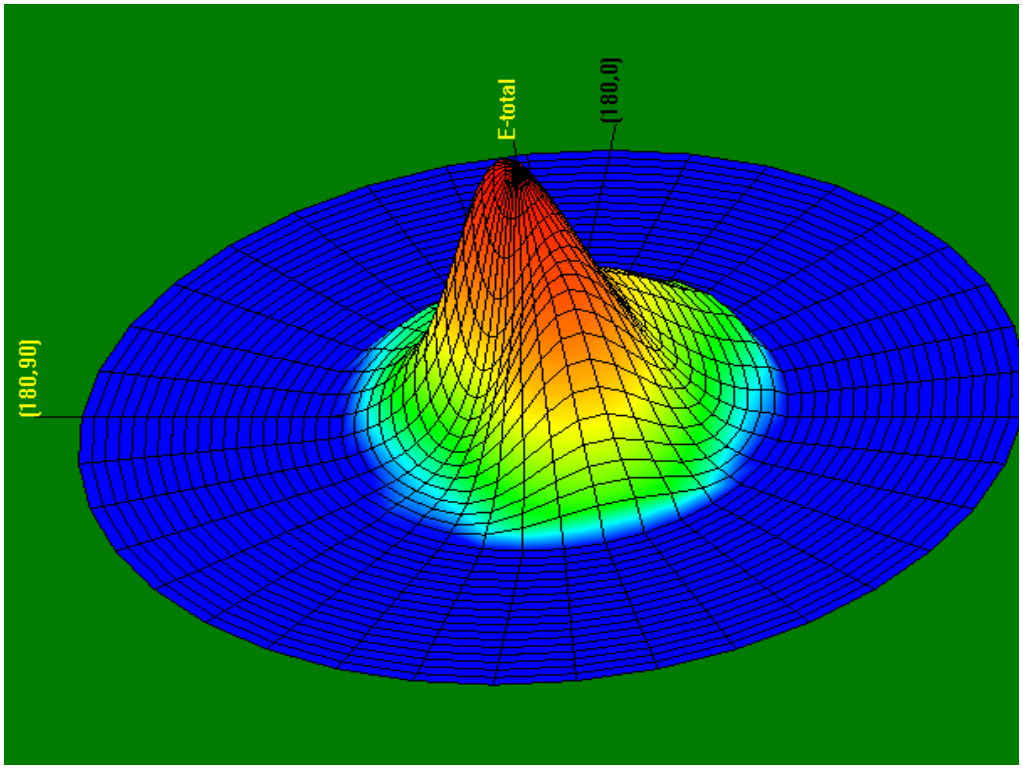

Figure7.11 ***Radiation Pattern of the Simulated Microstrip Antenna with decreased angle (mapped 3d view)***

8 CONCLUSIONS

In the present project work the rectangular microstrip patch antenna has been analyzed and broadband V-shaped rectangular microstrip antenna has been designed and simulated using IE3D software.

Following are the major conclusions of the present study

- The **Cavity Model** for the microstrip antenna has been studied in detail .
- Study of the method reveals that the cavity model is the most useful and popular model as compared to the full wave analysis which is more accurate but very complicated and doesn't give a good physical insight.
- The broadband V-shaped rectangular microstrip patch antenna has been successfully designed using conventional methods for a particular set of parameters.
- The evaluation version of **IE3D software by Zeland Software, Inc., USA** has been studied and used successfully to model and simulate the broadband V-shaped rectangular microstrip patch antenna.
- The results obtained from the simulations are found to be very close to the designed parameters.
- Radiation takes place in the **broadside direction** (z direction) as per the theoretical expectations. The microstrip patch lies on the x-y plane.
- The resonant frequency of the antenna is found to be **2.4 GHz** that lies within the bandwidth for which the antenna is designed.
- The gain is maximum at **2.4GHz**, which lies very near to the theoretical resonant frequency.
- Improved radiation pattern is obtained when angle of V-shaped patch is decreased.

9 SCOPE OF FURTHER STUDY

Results obtained in the designed antenna can be further improved. Back lobe occurring should be removed completely for practical antenna. S-parameter graph can also be improved simultaneously, which as a result further improve the other parameter graph.

In the present study the Cavity Model has been adopted for its advantages over other methods. There various methods of analyzing the microstrip antenna like the transmission line model, cavity model and full wave analysis method, which can be used in designing other microstrip antennas.

Different methods of analysis of the microstrip patch antenna can be studied for a wide range of frequencies. The results obtained from them can be compared and an optimum design method can be recommended.

In the present study coaxial probe feeding technique is used. Microstrip antenna with other feeding techniques can be designed and a comparative study can be done.

Study of different feeding techniques can be performed and the best feeding technique can therefore be worked out.

Different types of Microstrip antennas can be designed such as rectangular microstrip antenna, circular microstrip antenna, slotted microstrip antenna, etc. and a comparative study can be done to select optimum design

10 REFERENCES

1. **Bahl, I.J. and Bhartia, P.** , *Microstrip Antenna*, Artech House.
2. **Constantine, A. Balanis**, *Antenna Theory,* John Wiley Publication.
3. **Carver,K.R. , and J.W.Mink,** *Microstrip Antenna Technology*, IEEE Trans. Ants. Prop., AP-29, 25-38, January 1981.
4. **Derneryd, A.** , *A Theoretical Investigation of the Rectangular Microstrip Antenna element*, IEEE Trans. Ants. Prop. , AP-26, 532-535, July 1978.
5. **Munson, R.E.** , *Microstrip Antennas*, Antenna Engineering Handbook, McGraw Hill, 1984, Chap. 7.
6. **Pozar, D.M.**, *An Update on Microstrip Antenna Theory and Design Including Some Novel Feeding Techniques***,** IEEE Ants. Prop. Soc. Newsletter, 28, 5-9 October 1986.
7. **R. F. Harrington**, *Field Computation by Moment Method*, R E Kriegger Publishing Company, Malabar, Florida.
8. **Ramesh Garg, Prakash Bhartia, Inder Bahl, Apisak Ittipiboon,** *Microstrip Antenna Design Handbook,* Artech House, Boston.
9. **T. C. Edward, F***oundations of Microwave Integrated Circuits,* John Wiley Publication.
10. **IE3D User's Manual***,* Release 10.1, *Zeland Software*, Inc., Fremont, USA.